Spectral analysis of matrices in Galerkin methods based on generalized B-splines with high smoothness

Numerische Mathematik manuscript No.
(will be inserted by the editor)

Spectral analysis of matrices in Galerkin methods based on generalized B-splines with high smoothness

Fabio Roman · Carla Manni · Hendrik Speleers

Received: date / Accepted: date

Abstract We present a first step towards the spectral analysis of matrices arising from IgA Galerkin methods based on hyperbolic and trigonometric GB-splines. Second order differential problems with constant coefficients are considered and discretized by means of sequences of both nested and non-nested spline spaces. We prove that there always exists an asymptotic eigenvalue distribution which can be compactly described by a symbol, just like in the polynomial case. There is a complete similarity between the symbol expressions in the hyperbolic, trigonometric and polynomial cases. This results in similar spectral features of the corresponding matrices. We also analyze the IgA discretization based on trigonometric GB-splines for the eigenvalue problem related to the univariate Laplace operator. We prove that, for non-nested spaces, the phase parameter can be exploited to improve the spectral approximation with respect to the polynomial case. As part of the analysis, we derive several Fourier properties of cardinal GB-splines.

Mathematics Subject Classification (2010) 15A18 · 65N30 · 41A15 · 15B05 · 65L10

1 Introduction

Isogeometric Analysis (IgA) is a technology introduced nearly a decade ago in a seminal paper by Hughes et al. [19] that unifies Computer Aided Design (CAD) and Finite Element Analysis (FEA). CAD software, used in industry for geometric modeling, typically describes physical domains by means of tensor-product B-splines or Non-Uniform Rational B-Splines (NURBS). Such geometries are then further processed in the analysis phase. One of the key concepts in IgA is to use the same discretization and representation tools for the design as well as for the analysis (in an isoparametric environment), providing a

F. Roman
Department of Mathematics, University of Turin
Via Carlo Alberto 10, 10123 Torino, Italy
E-mail: fabio.roman@unito.it

C. Manni, H. Speleers
Department of Mathematics, University of Rome 'Tor Vergata'
Via della Ricerca Scientifica, 00133 Roma, Italy
E-mail: manni@mat.uniroma2.it; speleers@mat.uniroma2.it

true design-through-analysis methodology [7,19]. The isogeometric approach based on B-splines/NURBS results in some important advantages with respect to classical finite element approaches. The geometry of the physical domain is exactly described, so the interaction with the CAD system during any further refinement process in the analysis phase is eliminated. In addition, B-spline and NURBS spaces possess an inherent higher smoothness than those in classical FEA, leading to a higher accuracy per degree-of-freedom [3]. The success of IgA roots in the above properties, and this technology has been shown to be superior in various engineering application fields.

Even though NURBS are the de facto standard in CAD systems, they suffer from a few major drawbacks. For example, they lack an exact description of transcendental curves of interest in applications, and their parameterization of conic sections does not correspond to the arc length. In addition, NURBS behave poorly with respect to differentiation and integration, which are crucial operators in analysis.

The so-called Generalized B-splines (GB-splines) are smooth functions belonging piecewisely to more general spaces than algebraic polynomial spaces. Suitable selections of such section spaces – typically including polynomial and hyperbolic/trigonometric functions – allow for an exact representation of polynomial curves, conic sections, helices and other profiles of salient interest in applications. In particular, conic sections are exactly parameterized by hyperbolic/trigonometric generalized splines with respect to the arc length. GB-splines possess all fundamental properties of classical (polynomial) B-splines; we highlight their recurrence relation, minimum support and local linear independence. Moreover, contrarily to NURBS, they behave completely similar to B-splines with respect to differentiation and integration. For more details we refer to [6,22,23] and references therein.

Thanks to their structural similarity with (polynomial) B-splines, GB-splines are plug-to-plug compatible with B-splines in IgA. Moreover, their section spaces can be selected according to a problem-oriented strategy taking into account the geometrical and/or analytical peculiar issues of the specific addressed problem. The fine-tuning of the section spaces generally results in a gain from the accuracy point of view. These two aspects make hyperbolic and trigonometric GB-splines a flexible and interesting tool in IgA approximation methods [23,24,25]. Other main application areas of GB-splines are computer aided geometric design [4,35] and signal processing [34].

The Galerkin formulation has been intensively employed in the IgA context. Like any discretization technique, isogeometric Galerkin methods require to solve large linear systems. It turns out, however, that iterative solvers like classical multigrid methods are not always effective in this context (as illustrated and explained in [9]).

The spectral behavior of matrices arising from IgA discretization methods with (polynomial) B-splines has been deeply analyzed in a recent sequel of papers [11,14,15]. This spectral analysis is based on the notion of a spectral symbol, and exploits the properties of Generalized Locally Toeplitz (GLT) sequences [28,29] and of the B-spline basis. Such a spectral information plays a fundamental role in the convergence analysis of (preconditioned) Krylov methods (see, e.g., [2,21] and references therein) and is even more important in the design and in the theoretical analysis of effective preconditioners [27,30] and fast multigrid solvers [1]. In the IgA context with B-splines, the obtained spectral information has been exploited in [9,10] for devising optimal and totally robust multigrid solvers. The spectral symbol also provides a theoretical tool to analyze the spectral results obtained solving discrete generalized eigenvalue problems [13].

In this paper we present a first step towards the spectral analysis of matrices arising from IgA Galerkin methods based on GB-splines by addressing mainly the one-dimensional setting, with constant coefficients and no geometry map. Like in the (polynomial) B-spline

case, these one-dimensional results are crucial building blocks in the treatment of the multivariate problem [14]. Indeed, thanks to the tensor-product structure of the approximation spaces, the univariate results can be directly extended to the multivariate setting, see Section 6. It is likely that the spectral distribution of GB-spline discretization matrices corresponding to the general multivariate setting, with non-constant coefficients and geometry maps, can be addressed with similar techniques as those used in the polynomial case [15].

Because of their interest in practical applications, we mainly focus on hyperbolic and trigonometric GB-splines. We analyze the spectral behavior of the discretization matrices corresponding to a sequence of both nested and non-nested spaces. In particular, we prove that an asymptotic eigenvalue distribution always exists when the matrix-size tends to infinity and is compactly described by a symbol. Although the precise expressions of the symbols depend on the characteristics of the sequence of GB-spline spaces used in the discretization process, there is a complete similarity between the polynomial, hyperbolic and trigonometric cases. Therefore, the corresponding matrices possess similar spectral features: the presence of canonical small eigenvalues associated with low frequencies, but also the presence of small eigenvalues associated with high frequencies especially as the spline degree increases, see [11,12]. We point out that in the case of nested GB-spline spaces the corresponding symbols are exactly the same as in the case of (polynomial) B-spline spaces.

As a main consequence of the above results, we expect that the same techniques based on the symbol for the design of robust and optimal multigrid solvers derived in the polynomial spline case [9,10] can also be applied in the generalized spline setting as well.

In addition, we analyze the Galerkin IgA discretization based on trigonometric splines for the eigenvalue problem related to the univariate Laplace operator, a common problem considered in the IgA literature (see, e.g., [7,8,13,20]). It turns out that polynomial and trigonometric spline discretizations produce comparable approximations of the global spectrum, but the phase parameter of trigonometric splines is a flexible tool to locally improve the obtained approximation. In particular, if non-nested spaces are used, the phase parameter can be selected to minimize user specified measures of the relative spectral error.

All the results in this paper also hold for (polynomial) B-splines, as a limit configuration of both hyperbolic and trigonometric GB-splines. Therefore, the paper provides an extension of the spectral analysis recently presented in the B-spline literature [13,14], framing the polynomial case in a wider setting, and gives a further evidence of the structural similarities between polynomial, hyperbolic and trigonometric GB-splines.

The analysis carried out in this paper deeply relies on certain Fourier properties of (cardinal) GB-splines, which are not yet known in the literature. They are combined with the powerful theory of GLT sequences (also used in [13] and in a simplified form in [14]). This theory can be applied to any local discretization technique for differential problems [16,29], and turns out to be very effective in the IgA GB-spline setting.

The paper is organized as follows. Section 2 presents the univariate problem setting and provides some preliminaries on GB-splines and on the corresponding Galerkin discretizations. Section 3 is devoted to the definition and main properties of cardinal GB-splines and of some functions (which will play the role of symbols) based on them. These functions are used in Section 4 to describe the spectral distribution of the stiffness and mass matrices arising from Galerkin IgA discretizations based on hyperbolic and trigonometric splines, considering both nested and non-nested spaces. The Galerkin approximation of the eigenvalues of the univariate Laplace operator by means of trigonometric splines is addressed in Section 5, with a special focus on non-nested spaces and on the selection of their phase parameter. In Section 6 we study the spectral distribution of the stiffness matrices in the multivariate setting. Some concluding remarks are collected in Section 7.

2 Problem setting and preliminaries

In this section we describe our univariate model differential problems and the Galerkin approximation based on generalized spline spaces. To make the paper as self-contained as possible, we also briefly recall some definitions and theorems on spectral analysis which will be used later on to derive our main results.

2.1 Model problems

In this paper two univariate model problems are considered: a second order linear elliptic differential problem with constant coefficients and an eigenvalue problem for the Laplace operator.

2.1.1 Linear elliptic differential problem

As our first model problem we consider the following second order linear elliptic differential equation with constant coefficients and homogeneous Dirichlet boundary conditions:

$$\begin{cases} -u'' + \beta u' + \gamma u = \mathrm{f}, & 0 < x < 1, \\ u(0) = 0, \quad u(1) = 0, \end{cases} \tag{1}$$

with $\mathrm{f} \in L_2((0,1))$, $\beta \in \mathbb{R}$, $\gamma \geq 0$. The weak form of problem (1) reads as follows: find $u \in \mathcal{V} := H_0^1((0,1))$ such that

$$a(u,v) = \mathrm{F}(v), \quad \forall v \in \mathcal{V}, \tag{2}$$

where

$$a(u,v) := \int_0^1 (u'(x)v'(x) + \beta u'(x)v(x) + \gamma u(x)v(x))\,\mathrm{d}x, \quad \mathrm{F}(v) := \int_0^1 \mathrm{f}(x)v(x)\,\mathrm{d}x.$$

Following the Galerkin approach, we choose a finite dimensional subspace $\mathcal{W} \subset \mathcal{V}$ and we look for a function $u_{\mathcal{W}} \in \mathcal{W}$ such that

$$a(u_{\mathcal{W}}, v) = \mathrm{F}(v), \quad \forall v \in \mathcal{W}. \tag{3}$$

If we fix a basis $\{\varphi_1, \ldots, \varphi_N\}$ for $\mathcal{W}$ where $N := \dim \mathcal{W}$, then each element in $\mathcal{W}$ can be written as a linear combination of this basis. So, the Galerkin problem (3) is equivalent to finding a vector $\mathbf{u} \in \mathbb{R}^N$ such that

$$A\mathbf{u} = \mathbf{f}, \tag{4}$$

where $A := \left[a(\varphi_j, \varphi_i)\right]_{i,j=1}^N$ is the stiffness matrix and $\mathbf{f} := [\mathrm{F}(\varphi_i)]_{i=1}^N$. The matrix A is positive definite in the sense that $\mathbf{v}^T A\mathbf{v} > 0$, $\forall \mathbf{v} \in \mathbb{R}^N \backslash \{\mathbf{0}\}$. In particular, A is non-singular and so there exists a unique solution $\mathbf{u}$ of (4). Note that A is symmetric only when $\beta = 0$.

The matrix A can be decomposed into a sum of three matrices related to the diffusion, advection and reaction terms. More precisely, $A = K + \beta H + \gamma M$, where

$$K := \left[\int_0^1 \varphi_j'(x)\varphi_i'(x)\,\mathrm{d}x\right]_{i,j=1}^{N}, \tag{5}$$

$$H := \left[\int_0^1 \varphi_j'(x)\varphi_i(x)\,\mathrm{d}x\right]_{i,j=1}^{N}, \tag{6}$$

$$M := \left[\int_0^1 \varphi_j(x)\varphi_i(x)\,\mathrm{d}x\right]_{i,j=1}^{N}. \tag{7}$$

The matrices K and M are symmetric non-singular matrices and the matrix H is a skew-symmetric matrix.

In IgA the space $\mathcal{W}$ is usually chosen as a spline space with high (often maximal) continuity. In this paper we are going to construct the matrix A in the case where $\mathcal{W}$ is the space spanned by GB-splines. After the construction of the matrix A, we will study its spectral properties.

2.1.2 An eigenvalue problem

As our second model problem we consider the following eigenvalue problem for the univariate Laplace operator:

$$\begin{cases} -u'' = \omega^2 u, \quad 0 < x < 1, \\ u(0) = 0, \quad u(1) = 0, \end{cases} \tag{8}$$

whose non-trivial exact solutions are

$$u_k(x) := \sin(\omega_k x), \quad \omega_k := k\pi, \quad k = 1,2,\ldots$$

The weak form of problem (8) reads as follow: find non-trivial $u \in \mathcal{V}$ and ω^2 such that

$$\int_0^1 u'(x)v'(x)\,\mathrm{d}x - \omega^2 \int_0^1 u(x)v(x)\,\mathrm{d}x = 0, \quad \forall v \in \mathcal{V}.$$

Following the Galerkin approach, we choose a subspace $\mathcal{W}$ of $\mathcal{V}$ spanned by the basis $\{\varphi_1,\ldots,\varphi_N\}$, and using the same notation as in (4)–(7), we find approximate values $\omega^2_{\mathcal{W}}$ to ω^2 by solving

$$K\mathbf{u} = \omega^2_{\mathcal{W}} M\mathbf{u}.$$

This means that $\omega^2_{\mathcal{W}}$ is an eigenvalue of the matrix $L := M^{-1}K$. Therefore, the N eigenvalues of the matrix L, denoted by

$$\omega^2_{k,\mathcal{W}}, \quad k = 1,\ldots,N,$$

are an approximation of the first N eigenvalues of the problem (8), namely

$$\omega_k^2 = (k\pi)^2, \quad k = 1,\ldots,N. \tag{9}$$

In this paper we will consider a Galerkin discretization based on GB-splines and we will analyze the resulting approximate solution by means of the spectral properties of the matrices K and M already considered in the Galerkin discretization of (2).

2.2 GB-splines

For $p,n \geq 1$, we consider the uniform knot set

$$\{t_1,\dots,t_{n+2p+1}\} := \Big\{\underbrace{0,\dots,0}_{p+1},\frac{1}{n},\frac{2}{n},\dots,\frac{n-1}{n},\underbrace{1,\dots,1}_{p+1}\Big\}, \tag{10}$$

and the space

$$\mathbb{P}_p^{U,V} := \langle 1,x,\dots,x^{p-2},U(x),V(x)\rangle, \quad x \in [0,1]. \tag{11}$$

The functions $U,V \in C^{p-1}[0,1]$ are such that $\{U^{(p-1)},\ V^{(p-1)}\}$ is a Chebyshev system on $[t_i,t_{i+1}]$, i.e., any non-trivial element in the space $\langle U^{(p-1)},V^{(p-1)}\rangle$ has at most one zero in $[t_i,t_{i+1}]$, $i = p+1,\dots,p+n$. We denote by $\widetilde{U}_i,\widetilde{V}_i$ the unique elements in $\langle U^{(p-1)},V^{(p-1)}\rangle$ satisfying

$$\widetilde{U}_i(t_i) = 1,\ \widetilde{U}_i(t_{i+1}) = 0, \quad \widetilde{V}_i(t_i) = 0,\ \widetilde{V}_i(t_{i+1}) = 1, \quad i = p+1,\dots,p+n.$$

Popular examples of such a space (11) are

$$\mathbb{P}_p := \langle 1,x,\dots,x^{p-2},x^{p-1},x^p\rangle, \tag{12}$$

$$\mathbb{H}_{p,\alpha} := \langle 1,x,\dots,x^{p-2},\cosh(\alpha x),\sinh(\alpha x)\rangle, \quad 0 < \alpha \in \mathbb{R}, \tag{13}$$

$$\mathbb{T}_{p,\alpha} := \langle 1,x,\dots,x^{p-2},\cos(\alpha x),\sin(\alpha x)\rangle, \quad 0 < \alpha(t_{i+1}-t_i) < \pi. \tag{14}$$

We are interested in spaces of smooth functions belonging piecewisely to spaces of the form (11). Therefore, the space (11) is referred to as section space. The generalized spline space of degree p over the knot set (10) with sections in (11) is defined by

$$\mathcal{S}_{n,p}^{U,V} := \Big\{ s \in C^{p-1}([0,1]) :\ s|_{\left[\frac{i}{n},\frac{i+1}{n}\right)} \in \mathbb{P}_p^{U,V},\ i = 0,\dots,n-1 \Big\}. \tag{15}$$

Generalized spline spaces consisting of the particular section spaces (12), (13) and (14) are referred to as polynomial, hyperbolic (or exponential) and trigonometric spline spaces (with phase α), respectively.

Hyperbolic and trigonometric splines allow for an exact representation of conic sections as well as some transcendental curves (helix, cycloid, ...). They are attractive from a geometrical point of view. Indeed, they are able to provide parameterizations of conic sections with respect to the arc length so that equally spaced points in the parameter domain correspond to equally spaced points on the described curve.

For fixed values of the involved parameters, the spaces (13) and (14) have the same approximation power as the polynomial space $\mathbb{P}_p$, see [6, Section 3].

Definition 1 The GB-splines of degree p over the knot set (10) with sections in (11) are denoted by $N_{i,p}^{U,V} : [0,1] \to \mathbb{R}$, $i = 1,\dots,n+p$, and are defined recursively as follows[1]. For $p = 1$,

$$N_{i,1}^{U,V}(x) := \begin{cases} \widetilde{V}_i(x), & \text{if } x \in [t_i,t_{i+1}), \\ \widetilde{U}_{i+1}(x), & \text{if } x \in [t_{i+1},t_{i+2}), \\ 0, & \text{elsewhere,} \end{cases}$$

[1] The functions $N_{i,1}^{U,V}$ may also depend on p because of the definition of $\widetilde{U}_i$, $\widetilde{V}_i$, but we omit the parameter p in order to avoid a heavier notation. Moreover, in the most interesting cases (polynomial, hyperbolic and trigonometric GB-splines) the functions $N_{i,1}^{U,V}$ are independent of p.

and for $p \geq 2$,

$$N_{i,p}^{U,V}(x) := \delta_{i,p-1}^{U,V} \int_0^x N_{i,p-1}^{U,V}(s)\,\mathrm{d}s - \delta_{i+1,p-1}^{U,V} \int_0^x N_{i+1,p-1}^{U,V}(s)\,\mathrm{d}s,$$

where

$$\delta_{i,p}^{U,V} := \left(\int_0^1 N_{i,p}^{U,V}(s)\,\mathrm{d}s \right)^{-1}.$$

Fractions with zero denominators are considered to be zero, and $N_{i,p}^{U,V}(1) := \lim_{x \to 1^-} N_{i,p}^{U,V}(x)$.

It is well known (see, e.g., [23]) that the GB-splines $N_{1,p}^{U,V}, \ldots, N_{n+p,p}^{U,V}$ form a basis for the generalized spline space $\mathcal{S}_{n,p}^{U,V}$. The functions $N_{i,p}^{U,V}$ are non-negative and locally supported, namely

$$\operatorname{supp}(N_{i,p}^{U,V}) = [t_i, t_{i+p+1}], \quad i = 1, \ldots, n+p.$$

Moreover,

$$N_{i,p}^{U,V}(0) = N_{i,p}^{U,V}(1) = 0, \quad i = 2, \ldots, n+p-1.$$

For $p \geq 2$ the GB-splines $N_{i,p}^{U,V}$, $i = 1, \ldots, n+p$, form a partition of unity on $[0,1]$.

Remark 1 Hyperbolic and trigonometric GB-splines (with sections in the spaces (13) and (14), respectively) approach the classical (polynomial) B-splines of the same degree and over the same knot set when the phase parameter α approaches 0.

Remark 2 GB-splines can be defined in a more general setting than Definition 1. In particular, completely general knot sets can be considered and the section space can be chosen differently on each knot interval $[t_i, t_{i+1}]$; see, e.g., [23].

2.3 Galerkin GB-spline approximation

We approximate the weak solution u of our problems (1) and (8) by means of the Galerkin method, and we choose the approximation space $\mathcal{W}$ to be a space of smooth generalized spline functions as in (15) vanishing at the two ends of the unit interval. More precisely, for $p \geq 2$, $n \geq 1$ we set

$$\mathcal{W}_{n,p}^{U,V} := \left\{ s \in \mathcal{S}_{n,p}^{U,V} : s(0) = s(1) = 0 \right\}. \tag{16}$$

We have $\dim \mathcal{W}_{n,p}^{U,V} = n + p - 2$, and the space $\mathcal{W}_{n,p}^{U,V}$ is spanned by the set of GB-splines $\{N_{2,p}^{U,V}, \ldots, N_{n+p-1,p}^{U,V}\}$.

The stiffness matrix A in (4) identified by such a basis is the object of our interest and, from now onwards, will be denoted by $A_{n,p}^{U,V}$ in order to emphasize its dependence on n, p and on the functions U, V:

$$A_{n,p}^{U,V} := A = \left[a\left(N_{j+1,p}^{U,V}, N_{i+1,p}^{U,V} \right) \right]_{i,j=1}^{n+p-2}. \tag{17}$$

Due to the compact support of the GB-spline basis, the matrix $A_{n,p}^{U,V}$ has a $(2p+1)$-band structure. Referring to (5)–(7), we consider the following decomposition of the matrix,

$$A_{n,p}^{U,V} = nK_{n,p}^{U,V} + \beta H_{n,p}^{U,V} + \frac{\gamma}{n} M_{n,p}^{U,V},$$

where

$$nK_{n,p}^{U,V} := \left[\int_0^1 \left(N_{j+1,p}^{U,V}\right)'(x)\left(N_{i+1,p}^{U,V}\right)'(x)\,\mathrm{d}x\right]_{i,j=1}^{n+p-2}, \tag{18}$$

$$H_{n,p}^{U,V} := \left[\int_0^1 \left(N_{j+1,p}^{U,V}\right)'(x)\,N_{i+1,p}^{U,V}(x)\,\mathrm{d}x\right]_{i,j=1}^{n+p-2}, \tag{19}$$

$$\frac{1}{n}M_{n,p}^{U,V} := \left[\int_0^1 N_{j+1,p}^{U,V}(x)\,N_{i+1,p}^{U,V}(x)\,\mathrm{d}x\right]_{i,j=1}^{n+p-2}. \tag{20}$$

In view of the eigenvalue problem (8), we need to determine the values $\omega_{k,\mathcal{W}}^2$, $k = 1,\ldots,n+p-2$, as the eigenvalues of the matrix

$$L_{n,p}^{U,V} := n^2 (M_{n,p}^{U,V})^{-1} K_{n,p}^{U,V}. \tag{21}$$

The goal of this paper is to analyze the spectral properties of the matrices $A_{n,p}^{U,V}$ and $L_{n,p}^{U,V}$, mainly in the special case of hyperbolic and trigonometric splines.

2.4 Preliminaries on spectral analysis

For any matrix $X \in \mathbb{C}^{m\times m}$, $\sigma(X)$ is the collection of its eigenvalues and $\rho(X)$ is its spectral radius. The 2-norm of X is given by $\|X\| := \sqrt{\rho(X^*X)} = s_1(X)$, where $s_1(X)$ is the maximum singular value of X. The trace norm (or Schatten 1-norm of X) is given by $\|X\|_1 := \sum_{j=1}^m s_j(X)$, i.e., the sum of the singular values of the matrix. Since the number of non-zero singular values of X is precisely $\mathrm{rank}(X)$, it follows that, for all $X \in \mathbb{C}^{m\times m}$, $\|X\|_1 \le \mathrm{rank}(X)\|X\| \le m\|X\|$.

We now introduce some fundamental definitions and theorems for developing our spectral analysis. We first define the concept of (asymptotic) spectral distribution of a sequence of matrices. We denote by μ_d the Lebesgue measure in $\mathbb{R}^d$, and by $C_c(\mathbb{C},\mathbb{C})$ the space of continuous functions $F : \mathbb{C} \to \mathbb{C}$ with compact support.

Definition 2 Let $\{X_n\}$ be a sequence of matrices with strictly increasing dimension d_n, and let $f : D \to \mathbb{C}$ be a measurable function, with $D \subset \mathbb{R}^d$ measurable and such that $0 < \mu_d(D) < \infty$. We say that $\{X_n\}$ is distributed like f in the sense of the eigenvalues, and we write $\{X_n\} \sim_\lambda f$, if

$$\lim_{n\to\infty} \frac{1}{d_n}\sum_{j=1}^{d_n} F(\lambda_j(X_n)) = \frac{1}{\mu_d(D)}\int_D F(f(x_1,\ldots,x_d))\,\mathrm{d}x_1\cdots\mathrm{d}x_d, \quad \forall F \in C_c(\mathbb{C},\mathbb{C}).$$

The function f is referred to as the symbol of the sequence of matrices $\{X_n\}$.

Remark 3 The informal meaning behind the above definition is the following. If f is continuous and n is large enough then the spectrum of X_n behaves like a uniform sampling of f over D. For instance, if $d = 1$, $d_n = n$, and $D = [a,b]$, then the eigenvalues of X_n are approximately equal to $f(a + j(b-a)/n)$, $j = 1,\ldots,n$, for n large enough.

In the next definition we consider the concept of spectral clustering of a sequence of matrices at a subset of $\mathbb{C}$.

Definition 3 Let $\{X_n\}$ be a sequence of matrices with strictly increasing dimension, and let $S \subseteq \mathbb{C}$ be a non-empty closed subset of $\mathbb{C}$. We say that $\{X_n\}$ is strongly clustered at S if the following condition is satisfied:

$$\forall \varepsilon > 0, \quad \exists C_\varepsilon \text{ and } \exists n_\varepsilon : \quad \forall n \geq n_\varepsilon, \quad q_n(\varepsilon) \leq C_\varepsilon,$$

where $q_n(\varepsilon)$ is the number of eigenvalues of X_n lying outside the ε-expansion S_ε of S, i.e.,

$$S_\varepsilon := \bigcup_{s \in S} [\mathrm{Re}\, s - \varepsilon, \mathrm{Re}\, s + \varepsilon] \times [\mathrm{Im}\, s - \varepsilon, \mathrm{Im}\, s + \varepsilon].$$

The next theorem gives sufficient conditions for a sequence of matrices to have a given spectral distribution and to be strongly clustered [17].

Theorem 1 *Let $f : D \subset \mathbb{R}^d \to \mathbb{R}$ be a measurable function defined on the measurable set D with $0 < \mu_d(D) < \infty$. Let $\{X_n\}$ and $\{Y_n\}$ be two sequences of matrices with $X_n, Y_n \in \mathbb{C}^{d_n \times d_n}$, and $d_n < d_{n+1}$ for all n, such that*

- *X_n is Hermitian for all n;*
- *$\{X_n\} \sim_\lambda f$ and $\{X_n\}$ is strongly clustered at the essential range of f;*
- *there exists a constant C so that $\|X_n\|, \|Y_n\|_1 \leq C$ for all n.*

Set $Z_n := X_n + Y_n$. Then, $\{Z_n\} \sim_\lambda f$, and $\{Z_n\}$ is strongly clustered at the essential range of f.

A Toeplitz matrix is a square matrix whose entries are constant along each diagonal. Given a univariate function $f : [-\pi, \pi] \to \mathbb{R}$ belonging to $L_1([-\pi, \pi])$, we can associate to f a family (sequence) of Hermitian Toeplitz matrices $\{T_m(f)\}$ parameterized by the integer index m and defined for all $m \geq 1$ in the following way:

$$T_m(f) := \begin{bmatrix} \mathrm{f}_0 & \mathrm{f}_{-1} & \cdots & \cdots & \mathrm{f}_{-(m-1)} \\ \mathrm{f}_1 & \ddots & \ddots & & \vdots \\ \vdots & \ddots & \ddots & \ddots & \vdots \\ \vdots & & \ddots & \ddots & \mathrm{f}_{-1} \\ \mathrm{f}_{m-1} & \cdots & \cdots & \mathrm{f}_1 & \mathrm{f}_0 \end{bmatrix} \in \mathbb{C}^{m \times m},$$

where

$$\mathrm{f}_k := \frac{1}{2\pi} \int_{-\pi}^{\pi} f(\theta) \mathrm{e}^{-\mathrm{i}k\theta} \mathrm{d}\theta, \quad k \in \mathbb{Z},$$

are the Fourier coefficients of f. The function f is called the generating function of $T_m(f)$. The next theorem is one of the most important results concerning sequences of Toeplitz matrices. The second statement was originally proved by Szegö [18] and generalized in [32], by using linear algebra tools.

Theorem 2 *Let $f \in L_1([-\pi, \pi])$ be a real-valued function, and let $m_f := \mathrm{ess\,inf}\, f$, $M_f := \mathrm{ess\,sup}\, f$, and suppose $m_f < M_f$. Then,*

- *$\sigma(T_m(f)) \subset (m_f, M_f), \quad \forall m \geq 1$;*
- *$\{T_m(f)\} \sim_\lambda f$.*

Finally, we recall the following result about the 2-norm and the trace norm of Toeplitz matrices. This is a simplified version of [31, Corollary 4.2] where general Schatten q-norms of Toeplitz matrices are addressed.

Theorem 3 *If $f \in L_\infty([-\pi,\pi])$ then*

$$\|T_m(f)\| \leq \|f\|_{L_\infty([-\pi,\pi])}.$$

If $f \in L_1([-\pi,\pi])$ then

$$\|T_m(f)\|_1 \leq m\|f\|_{L_1([-\pi,\pi])}.$$

3 Cardinal GB-splines and symbols

In this section we focus on the space

$$\langle 1, t, \ldots, t^{p-2}, U(t), V(t)\rangle, \quad t \in [0,1], \tag{22}$$

where $U, V \in C^{p-1}[0, p+1]$ are such that $\{U^{(p-1)}, V^{(p-1)}\}$ is a Chebyshev system on $[0,1]$. We denote by $\widetilde{U}, \widetilde{V}$ the unique elements in the space $\langle U^{(p-1)}, V^{(p-1)}\rangle$ satisfying

$$\widetilde{U}(0) = 1,\ \widetilde{U}(1) = 0, \quad \widetilde{V}(0) = 0,\ \widetilde{V}(1) = 1. \tag{23}$$

Definition 4 The (normalized) cardinal GB-spline of degree $p \geq 1$ over the uniform knot set $\{0, 1, \ldots, p+1\}$ with sections in (22) is denoted by $\phi_p^{U,V}$ and is defined recursively as follows. For $p = 1$,

$$\phi_1^{U,V}(t) := \delta_1^{U,V} \begin{cases} \widetilde{V}(t), & \text{if t} \in [0,1), \\ \widetilde{U}(t-1), & \text{if t} \in [1,2), \\ 0, & \text{elsewhere,} \end{cases} \tag{24}$$

where $\delta_1^{U,V}$ is a normalization factor given by

$$\delta_1^{U,V} := \left(\int_0^1 \widetilde{V}(s)\,\mathrm{d}s + \int_1^2 \widetilde{U}(s-1)\,\mathrm{d}s\right)^{-1}.$$

For $p \geq 2$,

$$\phi_p^{U,V}(t) := \int_0^t (\phi_{p-1}^{U,V}(s) - \phi_{p-1}^{U,V}(s-1))\,\mathrm{d}s. \tag{25}$$

The cardinal GB-splines of degree p are the set of integer translates of $\phi_p^{U,V}$, namely $\{\phi_p^{U,V}(\cdot - k),\ k \in \mathbb{Z}\}$.

If the space (22) is the space of algebraic polynomials of degree less than or equal to p, i.e. $U(t) = t^{p-1}$ and $V(t) = t^p$, then the function defined in Definition 4 is the classical (polynomial) cardinal B-spline of degree p, denoted by ϕ_p. The properties of the cardinal GB-spline listed in the next subsection generalize those of ϕ_p; see, e.g., [14, Section 3.1].

3.1 Properties of cardinal GB-splines

The cardinal GB-spline $\phi_p^{U,V}$ is globally of class C^{p-1}, and possesses some fundamental properties. Many of them are well established in the literature (see, e.g., [23]), so we prove only the less known ones:

- *Positivity:*
$$\phi_p^{U,V}(t) > 0, \quad t \in (0, p+1).$$
- *Minimal support:*
$$\phi_p^{U,V}(t) = 0, \quad t \notin (0, p+1). \tag{26}$$
- *Partition of unity:*
$$\sum_{k\in\mathbb{Z}} \phi_p^{U,V}(t-k) = \sum_{k=1}^{p} \phi_p^{U,V}(k) = 1, \quad p \geq 2. \tag{27}$$
- *Recurrence relation for derivatives:*
$$(\phi_p^{U,V})^{(r)}(t) = (\phi_{p-1}^{U,V})^{(r-1)}(t) - (\phi_{p-1}^{U,V})^{(r-1)}(t-1), \quad 1 \leq r \leq p-1. \tag{28}$$
Proof Differentiating once the recurrence formula gives
$$(\phi_p^{U,V})^{(1)}(s) = \phi_{p-1}^{U,V}(s) - \phi_{p-1}^{U,V}(s-1).$$
The formula (28) simply follows by differentiating r times. □
- *Conditional symmetry with respect to* $\frac{p+1}{2}$:
$$\phi_p^{U,V}\left(\frac{p+1}{2}+t\right) = \phi_p^{U,V}\left(\frac{p+1}{2}-t\right) \quad \text{if} \quad \phi_1^{U,V}(1+t) = \phi_1^{U,V}(1-t). \tag{29}$$
Proof For $p = 1$ there is nothing to prove. We proceed by induction on p. By using the recurrence formula in (25), we get
$$\phi_p^{U,V}\left(\frac{p+1}{2}+t\right) - \phi_p^{U,V}\left(\frac{p+1}{2}-t\right) =$$
$$\int_0^{\frac{p+1}{2}+t} \phi_{p-1}^{U,V}(s) - \phi_{p-1}^{U,V}(s-1)\,\mathrm{d}s - \int_0^{\frac{p+1}{2}-t} \phi_{p-1}^{U,V}(s) - \phi_{p-1}^{U,V}(s-1)\,\mathrm{d}s =$$
$$\int_{\frac{p+1}{2}-t}^{\frac{p+1}{2}+t} \phi_{p-1}^{U,V}(s) - \phi_{p-1}^{U,V}(s-1)\,\mathrm{d}s = 0.$$
The last equality follows from the induction hypothesis that $\phi_{p-1}^{U,V}$ is symmetric with respect to $p/2$. □
- *Convolution relation:*
$$\phi_p^{U,V}(t) = (\phi_{p-1}^{U,V} * \phi_0)(t) := \int_{\mathbb{R}} \phi_{p-1}^{U,V}(t-s)\phi_0(s)\,\mathrm{d}s = \int_0^1 \phi_{p-1}^{U,V}(t-s)\,\mathrm{d}s, \quad p \geq 2, \tag{30}$$
where $\phi_0(t) := \chi_{[0,1)}(t)$. Moreover,
$$\phi_p^{U,V}(t) = \Big(\phi_1^{U,V} * \underbrace{\phi_0 * \cdots * \phi_0}_{p-1}\Big)(t), \quad \phi_p(t) = \Big(\underbrace{\phi_0 * \cdots * \phi_0}_{p+1}\Big)(t), \quad p \geq 1. \tag{31}$$

Proof By comparing the recurrence formula (25) with the relation (30), it is equivalent to prove that

$$\int_0^1 \phi_{p-1}^{U,V}(t-s)\,\mathrm{d}s = \int_0^t \left(\phi_{p-1}^{U,V}(s) - \phi_{p-1}^{U,V}(s-1)\right)\mathrm{d}s.$$

Moreover, for every f integrable, it holds

$$\int_0^1 f(t-s)\,\mathrm{d}s - \int_0^t (f(s) - f(s-1))\,\mathrm{d}s = \int_{-1}^0 f(s)\,\mathrm{d}s.$$

The GB-spline has its support contained in the positive semi-axis (see (26)), so we have $\int_{-1}^0 \phi_{p-1}^{U,V}(s)\,\mathrm{d}s = 0$, which completes the proof of (30). Since $\phi_1(t) = \phi_0(t) * \phi_0(t)$ and applying recursively (30), we immediately get the relations in (31). □

– *Inner products:*

$$\int_{\mathbb{R}} \phi_{p_1}^{U_1,V_1}(t)\,\phi_{p_2}^{U_2,V_2}(t+k)\,\mathrm{d}t = \Big(\phi_1^{U_1,V_1} * \phi_1^{U_2,V_2} * \underbrace{\phi_0 * \cdots * \phi_0}_{p_1+p_2-2}\Big)(p_2+1-k), \quad (32)$$

if $\phi_1^{U_2,V_2}(1+t) = \phi_1^{U_2,V_2}(1-t)$. In particular,

$$\int_{\mathbb{R}} \phi_{p_1}^{U,V}(t)\,\phi_{p_2}(t+k)\,\mathrm{d}t = \Big(\phi_1^{U,V} * \underbrace{\phi_0 * \cdots * \phi_0}_{p_1+p_2}\Big)(p_2+1-k) = \phi_{p_1+p_2+1}^{U,V}(p_2+1-k),$$

$$\int_{\mathbb{R}} \phi_{p_1}(t)\,\phi_{p_2}(t+k)\,\mathrm{d}t = \Big(\underbrace{\phi_0 * \cdots * \phi_0}_{p_1+p_2+2}\Big)(p_2+1-k) = \phi_{p_1+p_2+1}(p_2+1-k).$$

Proof These results follow immediately from the symmetry property (29) and the convolution relation (31) of cardinal GB-splines. More precisely,

$$\begin{aligned}\int_{\mathbb{R}} \phi_{p_1}^{U_1,V_1}(t)\,\phi_{p_2}^{U_2,V_2}(t+k)\,\mathrm{d}t &= \int_{\mathbb{R}} \phi_{p_1}^{U_1,V_1}(t)\,\phi_{p_2}^{U_2,V_2}(p_2+1-t-k)\,\mathrm{d}t \\ &= \left(\phi_{p_1}^{U_1,V_1} * \phi_{p_2}^{U_2,V_2}\right)(p_2+1-k) \\ &= \Big(\phi_1^{U_1,V_1} * \underbrace{\phi_0 * \cdots * \phi_0}_{p_1-1} * \phi_1^{U_2,V_2} * \underbrace{\phi_0 * \cdots * \phi_0}_{p_2-1}\Big)(p_2+1-k),\end{aligned}$$

which implies (32). □

– *Unity of integral:*

$$\int_0^{p+1} \phi_p^{U,V}(t)\,\mathrm{d}t = 1. \quad (33)$$

Proof For $p = 1$ it is true by construction. We proceed by induction on p. For $p \geq 2$ we set

$$\delta_p^{U,V} := \left(\int_{\mathbb{R}} \phi_p^{U,V}(t)\,\mathrm{d}t\right)^{-1},$$

and we need to prove that $\delta_p^{U,V} = 1$, which is equivalent to (33) due to the local support property (26). Using the convolution relation (30) we can write

$$(\delta_p^{U,V})^{-1} = \int_{\mathbb{R}} \phi_p^{U,V}(t)\,\mathrm{d}t = \int_{\mathbb{R}} \int_0^1 \phi_{p-1}^{U,V}(t-s)\,\mathrm{d}s\mathrm{d}t.$$

Thanks to the local support of the cardinal GB-spline, we can swap the order of the integrals and we get

$$(\delta_p^{U,V})^{-1} = \int_0^1 \int_{\mathbb{R}} \phi_{p-1}^{U,V}(t-s)\,\mathrm{d}t\mathrm{d}s = \int_0^1 \int_{\mathbb{R}} \phi_{p-1}^{U,V}(z)\,\mathrm{d}z\mathrm{d}s.$$

From the definition of $\delta_p^{U,V}$ and the inductive hypothesis, it follows that

$$(\delta_p^{U,V})^{-1} = \int_0^1 (\delta_{p-1}^{U,V})^{-1}\,\mathrm{d}s = 1.$$

□

In the following, we will focus in particular on hyperbolic and trigonometric cardinal GB-splines with real phase parameters α. The hyperbolic cardinal GB-spline is denoted by $\phi_p^{\mathbb{H}_\alpha}$ and is defined by taking $U(t) := \cosh(\alpha t)$ and $V(t) := \sinh(\alpha t)$. In this case, we have

$$\widetilde{U}(t) = \frac{\sinh(\alpha(1-t))}{\sinh(\alpha)}, \quad \widetilde{V}(t) = \frac{\sinh(\alpha t)}{\sinh(\alpha)}, \tag{34}$$

satisfying (23). The trigonometric cardinal GB-spline is denoted by $\phi_p^{\mathbb{T}_\alpha}$ and is defined by taking $U(t) := \cos(\alpha t)$ and $V(t) := \sin(\alpha t)$. In this case, we have

$$\widetilde{U}(t) = \frac{\sin(\alpha(1-t))}{\sin(\alpha)}, \quad \widetilde{V}(t) = \frac{\sin(\alpha t)}{\sin(\alpha)}, \tag{35}$$

satisfying (23). To simplify the notation, we will also use the notation $\phi_p^{\mathbb{Q}_\alpha}$ if a statement holds for both $\phi_p^{\mathbb{H}_\alpha}$ and $\phi_p^{\mathbb{T}_\alpha}$, but not necessarily for an arbitrary $\phi_p^{U,V}$.

Remark 4 Referring to Remark 1, hyperbolic and trigonometric cardinal GB-splines approach the (polynomial) cardinal B-spline of the same degree as the phase parameter α approaches 0, i.e.,

$$\lim_{\alpha\to 0} \phi_p^{\mathbb{Q}_\alpha}(t) = \phi_p(t), \quad \mathbb{Q} = \mathbb{H}, \mathbb{T}.$$

Remark 5 The symmetry requirement $\phi_1^{U,V}(1+t) = \phi_1^{U,V}(1-t)$ in (29) is equivalent to

$$\widetilde{V}(t) = \widetilde{U}(1-t), \quad t \in [0,1].$$

This requirement is satisfied for hyperbolic and trigonometric cardinal GB-splines, see (34)–(35), as well as for (polynomial) cardinal B-splines.

Remark 6 Taking into account the local support (26) and the unity of integral (33), we see that Definition 4 is in agreement with Definition 1 for $p \geq 2$. In particular, let

$$\{N_{i,p}^{\mathbb{Q}_\alpha} : i = 1, \ldots, n+p\}, \quad \mathbb{Q} = \mathbb{H}, \mathbb{T},$$

be a set of either hyperbolic or trigonometric GB-splines of degree p defined over the knot set (10) with sections in either (13) or (14), respectively. Then we have

$$N_{i,p}^{\mathbb{Q}_\alpha}(x) = \phi_p^{\mathbb{Q}_{\alpha/n}}(nx - i + p + 1), \quad i = p+1, \ldots, n, \quad p \geq 2.$$

This equality does not hold for $p = 1$ because of the integral normalization factor $\delta_1^{U,V}$ in (24). However, this normalization factor ensures that the convolution relation (30) holds for all cardinal GB-splines.

3.2 Fourier transform of cardinal GB-splines

The Fourier transform of $\phi_0(t) := \chi_{[0,1)}(t)$ is given by

$$\widehat{\phi_0}(\theta) = \frac{1 - \mathrm{e}^{-\mathrm{i}\theta}}{\mathrm{i}\theta},$$

and by using the convolution relation (31), we can write the Fourier transform of the cardinal GB-spline $\phi_p^{U,V}$ as

$$\widehat{\phi_p^{U,V}}(\theta) = \widehat{\phi_1^{U,V}}(\theta) \left(\frac{1 - \mathrm{e}^{-\mathrm{i}\theta}}{\mathrm{i}\theta}\right)^{p-1}. \tag{36}$$

Moreover, for the hyperbolic case, it can be checked that

$$\widehat{\phi_1^{\mathbb{H}_\alpha}}(\theta) = \left(\frac{\alpha^2}{\cosh(\alpha) - 1}\right)\left(\frac{\cosh(\alpha) - \cos(\theta)}{\theta^2 + \alpha^2}\right)\mathrm{e}^{-\mathrm{i}\theta}, \quad \alpha \in \mathbb{R}, \tag{37}$$

and for the trigonometric case,

$$\widehat{\phi_1^{\mathbb{T}_\alpha}}(\theta) = \left(\frac{\alpha^2}{1 - \cos(\alpha)}\right)\left(\frac{\cos(\alpha) - \cos(\theta)}{\theta^2 - \alpha^2}\right)\mathrm{e}^{-\mathrm{i}\theta}, \quad \alpha \in (0, \pi), \tag{38}$$

in which, if $\theta = \alpha$, we take the limit $\theta \to \alpha$. Note that

$$\widehat{\phi_1}(\theta) = \left(\frac{1 - \mathrm{e}^{-\mathrm{i}\theta}}{\mathrm{i}\theta}\right)^2 = 2\left(\frac{1 - \cos(\theta)}{\theta^2}\right)\mathrm{e}^{-\mathrm{i}\theta} = \lim_{\alpha \to 0} \widehat{\phi_1^{\mathbb{Q}_\alpha}}(\theta), \tag{39}$$

which is in agreement with Remark 4.

We now provide some lower bounds on the modulus of the Fourier transforms of the hyperbolic and trigonometric cardinal GB-splines, which will be useful later on.

Lemma 1 *We have*

$$\left|\widehat{\phi_p^{\mathbb{H}_\alpha}}(\theta)\right|^2 \geq \left(\frac{\alpha^2}{\cosh(\alpha) - 1}\right)^2 \left(\frac{\cosh(\alpha) + 1}{\pi^2 + \alpha^2}\right)^2 \left(\frac{4}{\pi^2}\right)^{p-1}, \tag{40}$$

and

$$\left|\widehat{\phi_p^{\mathbb{T}_\alpha}}(\theta)\right|^2 \geq \left(\frac{\alpha^2}{1 - \cos(\alpha)}\right)^2 \left(\frac{\cos(\alpha) + 1}{\pi^2 - \alpha^2}\right)^2 \left(\frac{4}{\pi^2}\right)^{p-1}. \tag{41}$$

Proof We just prove the hyperbolic case, because the trigonometric case can be addressed with similar arguments. From (37) we obtain

$$\left|\widehat{\phi_1^{\mathbb{H}_\alpha}}(\theta)\right|^2 \geq \left(\frac{\alpha^2}{\cosh(\alpha) - 1}\right)^2 \left(\frac{\cosh(\alpha) + 1}{\pi^2 + \alpha^2}\right)^2.$$

Moreover, since

$$|\widehat{\phi_0}(\theta)|^2 = \frac{2 - 2\cos(\theta)}{\theta^2} \geq \frac{4}{\pi^2},$$

we deduce the lower bound (40) from (36). □

Taking into account (39), for $\alpha \to 0$ the lower bounds (40)–(41) reduce to the lower bound for the polynomial case considered in [14, Eq. (24)].

3.3 Symbols

In this subsection we study the properties of the generating functions of some Toeplitz matrices which will play an important role in later sections.

We define the following functions in terms of cardinal GB-splines:

$$f_p^{U,V} : [-\pi,\pi] \to \mathbb{R}, \quad f_p^{U,V}(\theta) := \sum_{k=-p}^{p} \left(\int_{\mathbb{R}} \dot{\phi}_p^{U,V}(t)\, \dot{\phi}_p^{U,V}(t-k)\, \mathrm{d}t \right) \mathrm{e}^{\mathrm{i}k\theta}, \tag{42}$$

$$h_p^{U,V} : [-\pi,\pi] \to \mathbb{R}, \quad h_p^{U,V}(\theta) := \sum_{k=-p}^{p} \left(\int_{\mathbb{R}} \phi_p^{U,V}(t)\, \phi_p^{U,V}(t-k)\, \mathrm{d}t \right) \mathrm{e}^{\mathrm{i}k\theta}, \tag{43}$$

where $\dot{\phi}_p^{U,V}(t)$ denotes the derivative of $\phi_p^{U,V}(t)$ with respect to t. Note that both functions $f_p^{U,V}$ and $h_p^{U,V}$ are even real trigonometric polynomials. They can also be expressed in the following form

$$f_p^{U,V}(\theta) = \sum_{k=-p}^{p} \left(\int_{\mathbb{R}} \dot{\phi}_p^{U,V}(t)\, \dot{\phi}_p^{U,V}(t-k)\, \mathrm{d}t \right) \cos(k\theta),$$

$$h_p^{U,V}(\theta) = \sum_{k=-p}^{p} \left(\int_{\mathbb{R}} \phi_p^{U,V}(t)\, \phi_p^{U,V}(t-k)\, \mathrm{d}t \right) \cos(k\theta).$$

The corresponding functions in terms of (polynomial) cardinal B-splines are denoted by f_p and h_p (see also [14]), that is

$$f_p(\theta) := \sum_{k=-p}^{p} \left(\int_{\mathbb{R}} \dot{\phi}_p(t)\, \dot{\phi}_p(t-k)\, \mathrm{d}t \right) \mathrm{e}^{\mathrm{i}k\theta} = \sum_{k=-p}^{p} \left(\int_{\mathbb{R}} \dot{\phi}_p(t)\, \dot{\phi}_p(t-k)\, \mathrm{d}t \right) \cos(k\theta),$$

$$h_p(\theta) := \sum_{k=-p}^{p} \left(\int_{\mathbb{R}} \phi_p(t)\, \phi_p(t-k)\, \mathrm{d}t \right) \mathrm{e}^{\mathrm{i}k\theta} = \sum_{k=-p}^{p} \left(\int_{\mathbb{R}} \phi_p(t)\, \phi_p(t-k)\, \mathrm{d}t \right) \cos(k\theta).$$

We also recall the following result from [5, Theorem 2.28].

Theorem 4 *Let $\psi \in L_2(\mathbb{R})$ and its Fourier transform $\widehat{\psi}$ satisfy*

$$\psi(t) = O(|t|^{-a}), \quad a > 1, \quad \text{as } |t| \to \infty, \tag{44}$$

and

$$\widehat{\psi}(\theta) = O(|\theta|^{-b}), \quad b > \frac{1}{2}, \quad \text{as } |\theta| \to \infty. \tag{45}$$

Then,

$$\sum_{k\in\mathbb{Z}} \left(\int_{\mathbb{R}} \psi(t-k)\overline{\psi(t)}\, \mathrm{d}t \right) \mathrm{e}^{\mathrm{i}k\theta} = \sum_{k\in\mathbb{Z}} |\widehat{\psi}(\theta + 2k\pi)|^2, \quad \forall \theta \in [-\pi,\pi]. \tag{46}$$

In the following, we will assume that U and V are chosen such that (44) and (45) are satisfied for both $\psi = \phi_p^{U,V}$ and $\psi = \dot{\phi}_p^{U,V}$. The hyperbolic case (34) and the trigonometric case (35) satisfy these conditions.

The next two lemmas provide some properties of the functions defined in (42) and (43).

Lemma 2 *Let $p \geq 2$ and let $h_p^{U,V}$ be defined as in (43). Then the following properties hold.*

1. $\forall \theta \in [-\pi, \pi]$,
$$h_p^{U,V}(\theta) = \sum_{k \in \mathbb{Z}} \left| \widehat{\phi_p^{U,V}}(\theta + 2k\pi) \right|^2. \tag{47}$$

2. *For* $\mathbb{Q} = \mathbb{H}, \mathbb{T}$,
$$\min_{\theta \in [-\pi,\pi]} h_p^{\mathbb{Q}_\alpha}(\theta) \geq C^{\mathbb{Q}_\alpha} \left(\frac{4}{\pi^2} \right)^{p-1}, \tag{48}$$
where
$$C^{\mathbb{H}_\alpha} := \left(\frac{\alpha^2}{\cosh(\alpha) - 1} \right)^2 \left(\frac{\cosh(\alpha) + 1}{\pi^2 + \alpha^2} \right)^2,$$
$$C^{\mathbb{T}_\alpha} := \left(\frac{\alpha^2}{1 - \cos(\alpha)} \right)^2 \left(\frac{\cos(\alpha) + 1}{\pi^2 - \alpha^2} \right)^2.$$

3.
$$\max_{\theta \in [-\pi,\pi]} h_p^{U,V}(\theta) = h_p^{U,V}(0) = 1. \tag{49}$$

Proof The first statement immediately follows from (43) and (46) with $\psi = \phi_p^{U,V}$. To obtain the second statement, we simply observe that from (47) we have
$$h_p^{U,V}(\theta) \geq \left| \widehat{\phi_p^{U,V}}(\theta) \right|^2.$$
Then the lower bound in (48) is obtained by means of (40)–(41). Finally, we prove the third statement. Combining (46), the partition of unity (27) and the unity of integral (33) gives
$$\begin{aligned} |h_p^{U,V}(\theta)| &\leq \sum_{k=-p}^{p} \left(\int_{\mathbb{R}} \phi_p^{U,V}(t)\, \phi_p^{U,V}(t-k)\, \mathrm{d}t \right) |\mathrm{e}^{\mathrm{i}k\theta}| \\ &= \sum_{k=-p}^{p} \int_0^{p+1} \phi_p^{U,V}(t)\, \phi_p^{U,V}(t-k)\, \mathrm{d}t \\ &= \int_0^{p+1} \phi_p^{U,V}(t) \sum_{k=-p}^{p} \phi_p^{U,V}(t-k)\, \mathrm{d}t = \int_0^{p+1} \phi_p^{U,V}(t)\, \mathrm{d}t = 1. \end{aligned}$$
Moreover, with the same line of arguments, it is easy to check that $h_p^{U,V}(0) = 1$. □

Remark 7 The properties stated in Lemma 2 extend to $h_1^{\mathbb{Q}_\alpha}$, $\mathbb{Q} = \mathbb{H}, \mathbb{T}$ as follows:

- the relation (47) holds for $h_1^{\mathbb{Q}_\alpha}$;
- the lower bound (48) holds for $h_1^{\mathbb{Q}_\alpha}$ because (40) and (41) are still valid;
- the partition of unity (27) does not hold for $p = 1$ in general, but $\max_{\theta \in [-\pi,\pi]} h_1^{\mathbb{Q}_\alpha}(\theta) = h_1^{\mathbb{Q}_\alpha}(0)$, and by direct computation we get the bounds
$$1 < h_1^{\mathbb{H}_\alpha}(0) \leq 1 + \frac{\alpha^4}{720}, \quad 1 < h_1^{\mathbb{T}_\alpha}(0) \leq 1 + \frac{\alpha^4}{\pi^4} \left(\frac{\pi^2}{8} - 1 \right).$$

Figure 1 (left) shows some examples of h_p, $h_p^{\mathbb{H}_\alpha}$ and $h_p^{\mathbb{T}_\alpha}$. In the following, we will also use the notation
$$m_{h_p^{\mathbb{Q}_\alpha}} := \min_{\theta \in [-\pi,\pi]} h_p^{\mathbb{Q}_\alpha}(\theta), \quad \mathbb{Q} = \mathbb{H}, \mathbb{T}.$$

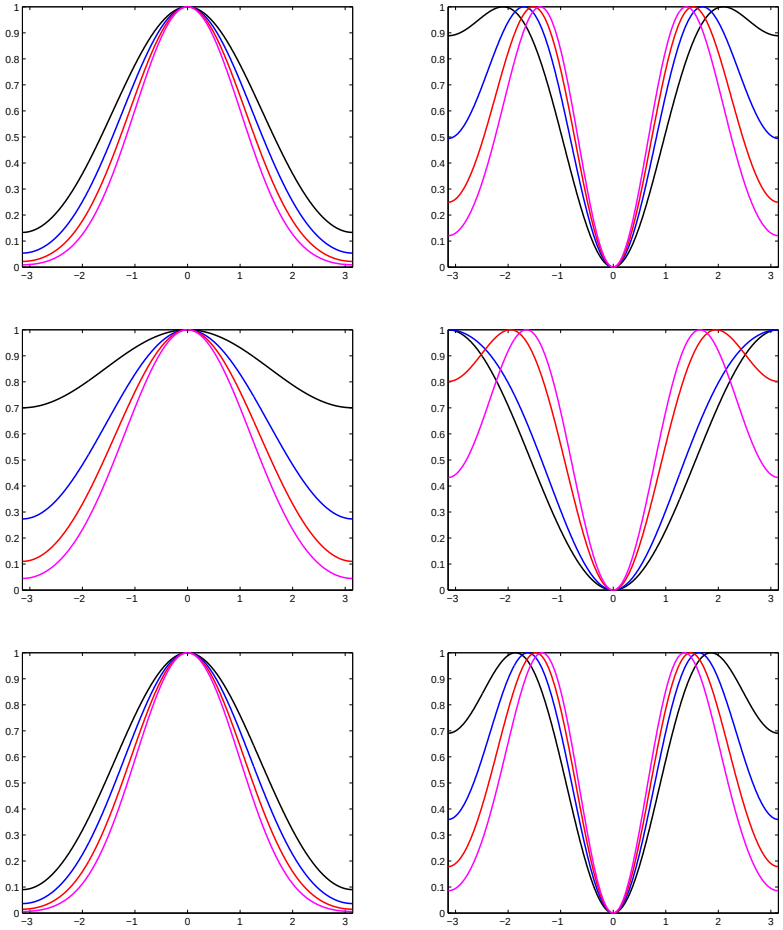

Fig. 1 From Top to Bottom. Left: plots of h_p, $h_p^{\mathbb{H}_{10}}$, $h_p^{\mathbb{T}_{\pi/2}}$. Right: normalized plots of f_p, $f_p^{\mathbb{H}_{10}}$, $f_p^{\mathbb{T}_{\pi/2}}$. Black: $p = 2$, blue: $p = 3$, red: $p = 4$, magenta: $p = 5$.

Lemma 3 *Let $p \geq 3$ and let $f_p^{U,V}$ be defined as in (42). Then the following properties hold.*

1. $\forall \theta \in [-\pi, \pi]$,

$$f_p^{U,V}(\theta) = (2 - 2\cos(\theta)) \sum_{k \in \mathbb{Z}} \left| \widehat{\phi_{p-1}^{U,V}}(\theta + 2k\pi) \right|^2 = (2 - 2\cos(\theta))\, h_{p-1}^{U,V}(\theta). \tag{50}$$

2. *For $\mathbb{Q} = \mathbb{H}, \mathbb{T}$,*

$$f_p^{\mathbb{Q}_\alpha}(\theta) \geq (2 - 2\cos(\theta))\, C^{\mathbb{Q}_\alpha} \left(\frac{4}{\pi^2} \right)^{p-2}, \tag{51}$$

$$f_p^{\mathbb{Q}_\alpha}(\theta) \leq \min \left(2 - 2\cos(\theta),\ (2 - 2\cos(\theta))^{p-1} \left(\frac{1}{\theta^{2p-4}} + \frac{1}{6\pi^{2p-6}} \right) \right), \tag{52}$$

where $C^{\mathbb{Q}_\alpha}$ is specified in (48).

3. $\min_{\theta\in[-\pi,\pi]} f_p^{\mathbb{Q}_\alpha}(\theta) = f_p^{\mathbb{Q}_\alpha}(0) = 0$, *and* $\theta = 0$ *is the unique zero of* $f_p^{\mathbb{Q}_\alpha}$ *over* $[-\pi,\pi]$.
4. $\max_{\theta\in[-\pi,\pi]} f_p^{\mathbb{Q}_\alpha}(\theta) \to 0$ *as* $p \to \infty$.

Proof The first equality in (50) can be proved as follows. From (36) we obtain for $p \geq 2$,

$$\widehat{\phi_p^{U,V}}(\theta) = \left(\frac{1-\mathrm{e}^{-\mathrm{i}\theta}}{\mathrm{i}\theta}\right)\widehat{\phi_{p-1}^{U,V}}(\theta),$$

and by using the derivative rule of the Fourier transform, we get

$$\widehat{\phi_p^{U,V}}(\theta) = \mathrm{i}\theta\,\widehat{\phi_p^{U,V}}(\theta) = (1-\mathrm{e}^{-\mathrm{i}\theta})\,\widehat{\phi_{p-1}^{U,V}}(\theta).$$

By taking squared moduli and summing, this yields

$$\sum_{k\in\mathbb{Z}}\left|\widehat{\phi_p^{U,V}}(\theta+2k\pi)\right|^2 = (2-2\cos(\theta))\sum_{k\in\mathbb{Z}}\left|\widehat{\phi_{p-1}^{U,V}}(\theta+2k\pi)\right|^2. \tag{53}$$

Then the first equality in (50) follows from (53) and (46) with $\psi = \phi_p^{U,V}$. The second equality can be immediately seen from (47).

Let us now consider the second statement. The lower bound in (51) follows from (50) and (48). Similarly, the upper bound $2-2\cos(\theta)$ in (52) follows from (50) and (49). For the other upper bound, we use the first expression of $f_p^{U,V}$ in (50) together with (36)–(37) for the hyperbolic case. More precisely, we have

$$\begin{aligned}\left|\widehat{\phi_{p-1}^{\mathbb{H}_\alpha}}(\theta+2k\pi)\right|^2 &= \left(\frac{2-2\cos(\theta)}{(\theta+2k\pi)^2}\right)^{p-2}\left(\frac{\alpha^2}{\cosh(\alpha)-1}\right)^2\left(\frac{\cosh(\alpha)-\cos(\theta)}{(\theta+2k\pi)^2+\alpha^2}\right)^2\\ &\leq \left(\frac{2-2\cos(\theta)}{(\theta+2k\pi)^2}\right)^{p-2},\end{aligned}$$

resulting in

$$f_p^{\mathbb{H}_\alpha}(\theta) \leq \sum_{k\in\mathbb{Z}}\frac{(2-2\cos(\theta))^{p-1}}{(\theta+2k\pi)^{2p-4}} \leq (2-2\cos(\theta))^{p-1}\left(\frac{1}{\theta^{2p-4}}+\frac{1}{6\pi^{2p-6}}\right).$$

The trigonometric case can be addressed with a similar computation.

The third statement follows from the inequalities in (51)–(52). Finally, from the upper bound in (52) we also obtain the fourth statement. □

Remark 8 The properties stated in Lemma 3 extend to $f_2^{\mathbb{Q}_\alpha}$, $\mathbb{Q} = \mathbb{H}, \mathbb{T}$ as follows:

- the relation (50) holds for $f_2^{\mathbb{Q}_\alpha}$;
- lower and upper bounds for $f_2^{\mathbb{Q}_\alpha}$ can be obtained by considering the relation $f_2^{\mathbb{Q}_\alpha}(\theta) = (2-2\cos(\theta))\,h_1^{\mathbb{Q}_\alpha}(\theta)$ together with the bounds for $h_1^{\mathbb{Q}_\alpha}$ given in Remark 7;
- the third statement holds for $f_2^{\mathbb{Q}_\alpha}$.

Taking into account (36) together with the explicit expressions in (37)–(39), formula (50) gives in the polynomial, hyperbolic and trigonometric case:

$$f_p(\theta) = \sum_{k\in\mathbb{Z}} \frac{(2-2\cos(\theta))^{p+1}}{(\theta+2k\pi)^{2p}}, \tag{54}$$

$$f_p^{\mathbb{H}_\alpha}(\theta) = \sum_{k\in\mathbb{Z}} \frac{(2-2\cos(\theta))^{p-1}}{(\theta+2k\pi)^{2p-4}} \left(\frac{\alpha^2}{\cosh(\alpha)-1}\right)^2 \left(\frac{\cosh(\alpha)-\cos(\theta)}{(\theta+2k\pi)^2+\alpha^2}\right)^2, \tag{55}$$

$$f_p^{\mathbb{T}_\alpha}(\theta) = \sum_{k\in\mathbb{Z}} \frac{(2-2\cos(\theta))^{p-1}}{(\theta+2k\pi)^{2p-4}} \left(\frac{\alpha^2}{1-\cos(\alpha)}\right)^2 \left(\frac{\cos(\alpha)-\cos(\theta)}{(\theta+2k\pi)^2-\alpha^2}\right)^2. \tag{56}$$

Figure 1 (right) shows some examples of f_p/M_{f_p}, $f_p^{\mathbb{H}_\alpha}/M_{f_p^{\mathbb{H}_\alpha}}$ and $f_p^{\mathbb{T}_\alpha}/M_{f_p^{\mathbb{T}_\alpha}}$, where

$$M_{f_p} := \max_{\theta\in[-\pi,\pi]} f_p(\theta), \quad M_{f_p^{\mathbb{Q}_\alpha}} := \max_{\theta\in[-\pi,\pi]} f_p^{\mathbb{Q}_\alpha}(\theta), \quad \mathbb{Q} = \mathbb{H}, \mathbb{T}.$$

Referring to Remark 4, the results provided in Lemmas 2 and 3 also hold in the polynomial case taking $\alpha \to 0$. Indeed, they generalize the results provided in [14, Lemmas 7 and 6]. From [14, Lemma 7] we recall that

$$\left(\frac{4}{\pi^2}\right)^{p+1} \le h_p(\theta) \le h_p(0) = 1,$$

and from [14, Eq. (28)] that

$$f_p(\theta) \ge (2-2\cos(\theta)) \left(\frac{4}{\pi^2}\right)^p, \tag{57}$$

$$f_p(\theta) \le \min\left(2-2\cos(\theta),\ (2-2\cos(\theta))^{p+1}\left(\frac{1}{\theta^{2p}} + \frac{1}{6\pi^{2p-2}}\right)\right). \tag{58}$$

Lemma 4 *The ratio $f_p^{\mathbb{Q}_\alpha}(\pi)/M_{f_p^{\mathbb{Q}_\alpha}}$, $\mathbb{Q} = \mathbb{H}, \mathbb{T}$ converges exponentially to zero as $p \to \infty$. In particular, for $p \ge 3$ it holds*

$$\frac{f_p^{\mathbb{H}_\alpha}(\pi)}{M_{f_p^{\mathbb{H}_\alpha}}} \le \frac{f_p^{\mathbb{H}_\alpha}(\pi)}{f_p^{\mathbb{H}_\alpha}(\pi/2)} \le \left(\frac{\cosh(\alpha)+1}{\pi^2+\alpha^2}\right)^2 \left(\frac{(\pi/2)^2+\alpha^2}{\cosh(\alpha)}\right)^2 \frac{\pi^2}{4} 2^{3-p},$$

$$\frac{f_p^{\mathbb{T}_\alpha}(\pi)}{M_{f_p^{\mathbb{T}_\alpha}}} \le \frac{f_p^{\mathbb{T}_\alpha}(\pi)}{f_p^{\mathbb{T}_\alpha}(\pi/2)} \le \left(\frac{\cos(\alpha)+1}{\pi^2-\alpha^2}\right)^2 \left(\frac{(\pi/2)^2-\alpha^2}{\cos(\alpha)}\right)^2 \frac{\pi^2}{4} 2^{3-p}.$$

Proof We just prove the hyperbolic case, because the trigonometric case can be addressed with similar arguments. From (55) we get

$$\begin{aligned} f_p^{\mathbb{H}_\alpha}\left(\frac{\pi}{2}\right) &= \frac{2^{3p-5}}{\pi^{2p-4}} \left(\frac{\alpha^2}{\cosh(\alpha)-1}\right)^2 \sum_{k\in\mathbb{Z}} \frac{1}{(4k+1)^{2p-4}} \left(\frac{\cosh(\alpha)}{(\pi/2+2k\pi)^2+\alpha^2}\right)^2 \\ &\ge \frac{2^{3p-5}}{\pi^{2p-4}} \left(\frac{\alpha^2}{\cosh(\alpha)-1}\right)^2 \left(\frac{\cosh(\alpha)}{(\pi/2)^2+\alpha^2}\right)^2, \end{aligned}$$

and

$$f_p^{\mathbb{H}_\alpha}(\pi) = \frac{2^{2p-2}}{\pi^{2p-4}}\left(\frac{\alpha^2}{\cosh(\alpha)-1}\right)^2 \sum_{k\in\mathbb{Z}} \frac{1}{(2k+1)^{2p-4}}\left(\frac{\cosh(\alpha)+1}{(\pi+2k\pi)^2+\alpha^2}\right)^2$$
$$\leq \frac{2^{2p-2}}{\pi^{2p-4}}\left(\frac{\alpha^2}{\cosh(\alpha)-1}\right)^2 \left(\frac{\cosh(\alpha)+1}{\pi^2+\alpha^2}\right)^2 \sum_{k\in\mathbb{Z}} \frac{1}{(2k+1)^{2p-4}}.$$

Since $\sum_{k\in\mathbb{Z}}(2k+1)^{-2p+4} \leq \sum_{k\in\mathbb{Z}}(2k+1)^{-2} = \frac{\pi^2}{4}$ for $p \geq 3$, we obtain the stated bound. □

The exponential convergence to zero of $f_p(\pi)$ was already observed in [12]. In particular, an exact relation was provided for the polynomial case:

$$f_p(\pi) = 2^{2-p} f_p(\pi/2), \quad p \geq 1. \tag{59}$$

Lemma 5 *For $p \geq 2$ and sufficiently large n, it holds*

$$\left\| f_p^{\mathbb{Q}_{\alpha/n}} - f_p \right\|_{L_1([-\pi,\pi])} \leq C\, n^{-2}, \quad \mathbb{Q} = \mathbb{H}, \mathbb{T}, \tag{60}$$

where C is a constant independent of n.

Proof We just prove the hyperbolic case, because the trigonometric case can be addressed with similar arguments. From (54)–(55) we obtain

$$\left| f_p^{\mathbb{H}_{\alpha/n}}(\theta) - f_p(\theta) \right| \leq (2-2\cos(\theta)) \sum_{k\in\mathbb{Z}} \left(\frac{2-2\cos(\theta)}{(\theta+2k\pi)^2}\right)^{p-2} \left| r^{\mathbb{H}}\left(\frac{\alpha}{n}, \theta+2k\pi\right)\right|,$$

where

$$r^{\mathbb{H}}(\varepsilon,\eta) := \left(\frac{\varepsilon^2}{\cosh(\varepsilon)-1}\right)^2 \left(\frac{\cosh(\varepsilon)-\cos(\eta)}{\eta^2+\varepsilon^2}\right)^2 - \left(\frac{2-2\cos(\eta)}{\eta^2}\right)^2.$$

We consider the Taylor expansion of $r^{\mathbb{H}}$ with respect to ε up to the second degree at the point 0, i.e.,

$$\varepsilon^2 \frac{(2-2\cos(\eta))(5\eta^2+(\eta^2+12)\cos(\eta)-12)}{3\eta^6} =: \varepsilon^2 \tilde{r}^{\mathbb{H}}(\eta).$$

It can be verified that $|\tilde{r}^{\mathbb{H}}(\eta)| \leq 8\min(1,\eta^{-4})$. As a consequence, we have for sufficiently small ε,

$$|r^{\mathbb{H}}(\varepsilon,\eta)| \leq \varepsilon^2 \widetilde{C} \min(1,\eta^{-4}),$$

for some positive constant $\widetilde{C}$ independent of ε and η. Moreover, we have

$$2-2\cos(\theta) \leq 4, \quad \frac{2-2\cos(\theta)}{(\theta+2k\pi)^2} \leq \frac{2-2\cos(\theta)}{\theta^2} \leq 1.$$

Using the previous bounds, we obtain for sufficiently large n,

$$\left| f_p^{\mathbb{H}_{\alpha/n}}(\theta) - f_p(\theta) \right| \leq 4\left(\left| r^{\mathbb{H}}\left(\frac{\alpha}{n},\theta\right)\right| + \sum_{k\neq 0} \left| r^{\mathbb{H}}\left(\frac{\alpha}{n},\theta+2k\pi\right)\right| \right)$$
$$\leq 4\left(\frac{\alpha}{n}\right)^2 \widetilde{C}\left(1+\sum_{k\neq 0}\frac{1}{(\theta+2k\pi)^4}\right)$$
$$\leq 4\left(\frac{\alpha}{n}\right)^2 \widetilde{C}\left(1+\frac{2}{\pi^4}\sum_{k\geq 1}\frac{1}{(2k-1)^4}\right) \leq \breve{C} n^{-2},$$

which implies (60). □

4 Spectral analysis in case of our linear differential problem

In this section we determine the (asymptotic) spectral distribution of the sequence of normalized matrices

$$\frac{1}{n} A_{n,p}^{U,V},$$

as the mesh size $1/n$ tends to zero. We only consider hyperbolic and trigonometric GB-spline discretizations because of their practical relevance. For the classical (polynomial) B-spline case we refer the reader to the spectral analysis in [14]. To simplify the notation, in agreement with the previous section, we denote by

$$\{N_{i,p}^{\mathbb{H}_\alpha} : i = 1,\dots,n+p\} \quad \text{and} \quad \{N_{i,p}^{\mathbb{T}_\alpha} : i = 1,\dots,n+p\}$$

the hyperbolic and trigonometric GB-splines of degree p defined over the knot set (10) with sections in (13) and (14), respectively. A completely similar notation will be used for the corresponding space (16) and the matrices in (17)–(20).

As already described in Remark 6, for $\mathbb{Q} = \mathbb{H}, \mathbb{T}$ the central basis functions $N_{i,p}^{\mathbb{Q}_\mu}, i = p+1,\dots,n$ can be expressed in terms of cardinal GB-splines, i.e.,

$$N_{i,p}^{\mathbb{Q}_\mu}(x) = \phi_p^{\mathbb{Q}_{\mu/n}}(nx - i + p + 1), \quad i = p+1,\dots,n, \quad p \geq 2, \tag{61}$$

and as a consequence,

$$(N_{i,p}^{\mathbb{Q}_\mu})'(x) = n\phi_p^{\mathbb{Q}_{\mu/n}}(nx - i + p + 1), \quad i = p+1,\dots,n, \quad p \geq 2. \tag{62}$$

In view of (61) two choices for the parameter μ are of interest when considering a sequence of spaces $\mathcal{W}_{n,p}^{\mathbb{Q}_\mu}$, $n \to \infty$.

- $\mu = \alpha$ where α is a given real value. This is the most natural choice for Galerkin IgA discretizations, because it generates a sequence of nested spaces $\mathcal{W}_{n,p}^{\mathbb{Q}_\alpha}$ given a sequence of nested knot sets. The basis functions in (61) are a scaled shifted version of a sequence of cardinal hyperbolic/trigonometric GB-splines identified by a sequence of parameters approaching 0 as n increases.
- $\mu = n\alpha$ where α is a given real value. In this case, the basis functions in (61) are a scaled shifted version of the same cardinal hyperbolic/trigonometric GB-spline for all n. The corresponding spaces $\mathcal{W}_{n,p}^{\mathbb{Q}_{n\alpha}}$ are not nested. Nevertheless, this discretization presents some advantages for the treatment of eigenvalue problems, see Section 5. Moreover, the analysis of the spectral properties of the sequence of matrices in (17) gives some interesting insights into the spectrum of the corresponding matrices in the above (nested) case for finite n, see Section 4.4.

In the following, we will address these two choices and will refer to them as the nested and non-nested case, respectively. We recall that the parameter μ is constrained by the Chebyshev structure of the section spaces (see (13) and (14)).

4.1 Galerkin matrices based on hyperbolic and trigonometric GB-splines

In view of the spectral analysis we intend to develop, we start by collecting some properties of the stiffness matrix (17) in case of hyperbolic and trigonometric GB-splines.

The central part of the matrix $A_{n,p}^{\mathbb{Q}_\mu}$ is only determined by the cardinal GB-splines involved in (61). More precisely, for each $k = 0, 1, \dots, p$ and $i = 2p, \dots, n-p-1$, the non-zero element in $A_{n,p}^{\mathbb{Q}_\mu}$ at row i and column $i \pm k$ can be expressed by

$$\begin{aligned}(A_{n,p}^{\mathbb{Q}_\mu})_{i,i\pm k} &= a(N_{i+1\pm k,p}^{\mathbb{Q}_\mu}(x), N_{i+1,p}^{\mathbb{Q}_\mu}(x)) \\ &= a(\phi_p^{\mathbb{Q}_{\mu/n}}(nx - i + p \mp k), \phi_p^{\mathbb{Q}_{\mu/n}}(nx - i + p)) \\ &= n(K_{n,p}^{\mathbb{Q}_\mu})_{i,i\pm k} + \beta(H_{n,p}^{\mathbb{Q}_\mu})_{i,i\pm k} + \frac{\gamma}{n}(M_{n,p}^{\mathbb{Q}_\mu})_{i,i\pm k}, \end{aligned} \tag{63}$$

where, from (18)–(20) and (61)–(62), we obtain for $k = 0, 1, \dots, p$ and $i = 2p, \dots, n-p-1$,

$$(K_{n,p}^{\mathbb{Q}_\mu})_{i,i\pm k} = \int_0^{p+1} \dot{\phi}_p^{\mathbb{Q}_{\mu/n}}(t \mp k)\dot{\phi}_p^{\mathbb{Q}_{\mu/n}}(t)\,\mathrm{d}t, \tag{64}$$

$$(H_{n,p}^{\mathbb{Q}_\mu})_{i,i\pm k} = \int_0^{p+1} \dot{\phi}_p^{\mathbb{Q}_{\mu/n}}(t \mp k)\phi_p^{\mathbb{Q}_{\mu/n}}(t)\,\mathrm{d}t, \tag{65}$$

$$(M_{n,p}^{\mathbb{Q}_\mu})_{i,i\pm k} = \int_0^{p+1} \phi_p^{\mathbb{Q}_{\mu/n}}(t \mp k)\phi_p^{\mathbb{Q}_{\mu/n}}(t)\,\mathrm{d}t. \tag{66}$$

The central rows of $A_{n,p}^{\mathbb{Q}_\mu}$ are defined as the rows with index ranging from $2p$ to $n-p-1$. These are the rows considered in (63). Since $A_{n,p}^{\mathbb{Q}_\mu}$ is of size $(n+p-2) \times (n+p-2)$, we have to require $n \geq 3p+1$ if we want to ensure there is at least one central row.

Following the same line of arguments as in [14, Section 4.4], for every $n \geq 3p+1$, we decompose the matrix $K_{n,p}^{\mathbb{Q}_\mu}$ into

$$K_{n,p}^{\mathbb{Q}_\mu} = B_{n,p}^{\mathbb{Q}_\mu} + R_{n,p}^{\mathbb{Q}_\mu}, \tag{67}$$

where $B_{n,p}^{\mathbb{Q}_\mu}$ is the symmetric $(2p+1)$-band Toeplitz matrix whose generic central row is given by (64). The matrix $R_{n,p}^{\mathbb{Q}_\mu} := K_{n,p}^{\mathbb{Q}_\mu} - B_{n,p}^{\mathbb{Q}_\mu}$ is a low-rank correction term. Indeed, $R_{n,p}^{\mathbb{Q}_\mu}$ has at most $2(2p-1)$ non-zero rows and so

$$\operatorname{rank}(R_{n,p}^{\mathbb{Q}_\mu}) \leq 2(2p-1). \tag{68}$$

In the next lemma we analyze the spectral properties of $B_{n,p}^{\mathbb{Q}_\mu}$.

Lemma 6 *For $p \geq 2$ and $n \geq 3p+1$, it holds*

$$B_{n,p}^{\mathbb{Q}_\mu} = T_{n+p-2}\big(f_p^{\mathbb{Q}_{\mu/n}}\big) \quad \textit{with} \quad \sigma(B_{n,p}^{\mathbb{Q}_\mu}) \subset \big(0, M_{f_p^{\mathbb{Q}_{\mu/n}}}\big), \quad \mathbb{Q} = \mathbb{H}, \mathbb{T}.$$

Proof From the definitions of $B_{n,p}^{\mathbb{Q}_\mu}$ and $f_p^{\mathbb{Q}_{\mu/n}}$ it follows that $B_{n,p}^{\mathbb{Q}_\mu} = T_{n+p-2}(f_p^{\mathbb{Q}_{\mu/n}})$ for any $n \geq 3p+1$. Hence, the statements are consequences of Theorem 2 and Lemma 3. □

We also recall that the matrix $K_{n,p}^{\mathbb{Q}_\mu}$ is symmetric, the matrix $H_{n,p}^{\mathbb{Q}_\mu}$ is skew-symmetric and the matrix $M_{n,p}^{\mathbb{Q}_\mu}$ is symmetric. The next lemma gives a bound for the infinity norm of these matrices. It extends the results in [14, Lemma 8] to the case of hyperbolic and trigonometric GB-splines.

Lemma 7 *For $p \geq 2$, it holds*

$$\left\|\frac{1}{n}M_{n,p}^{\mathbb{Q}_\mu}\right\|_\infty \leq \frac{p+1}{n}, \quad \left\|H_{n,p}^{\mathbb{Q}_\mu}\right\|_\infty \leq 2, \quad \left\|nK_{n,p}^{\mathbb{Q}_\mu}\right\|_\infty \leq C_{p,\alpha}\, n, \quad \mathbb{Q} = \mathbb{H}, \mathbb{T}, \quad \mu = \alpha, n\alpha,$$

where $C_{p,\alpha}$ is a constant independent of n.

Proof The knot set (10) implies that the maximum length of the support of any $N_{i,p}^{\mathbb{Q}_\mu}$ is $\frac{p+1}{n}$. By the positivity property and the partition of unity property of GB-splines, we obtain

$$\begin{aligned}
\left\|\frac{1}{n}M_{n,p}^{\mathbb{Q}_\mu}\right\|_\infty &= \max_{i=1,\dots,n+p-2} \sum_{j=1}^{n+p-2} \int_0^1 N_{j+1,p}^{\mathbb{Q}_\mu}(x)\, N_{i+1,p}^{\mathbb{Q}_\mu}(x)\,\mathrm{d}x \\
&= \max_{i=1,\dots,n+p-2} \int_0^1 \left(\sum_{j=1}^{n+p-2} N_{j+1,p}^{\mathbb{Q}_\mu}(x)\right) N_{i+1,p}^{\mathbb{Q}_\mu}(x)\,\mathrm{d}x \\
&\leq \max_{i=1,\dots,n+p-2} \int_0^1 N_{i+1,p}^{\mathbb{Q}_\mu}(x)\,\mathrm{d}x \leq \frac{p+1}{n}.
\end{aligned}$$

Since $H_{n,p}^{\mathbb{Q}_\mu}$ is skew-symmetric, its infinity norm is equal to the infinity norm of its transpose. Therefore, from Definition 1 we obtain

$$\begin{aligned}
\left\|H_{n,p}^{\mathbb{Q}_\mu}\right\|_\infty &= \max_{i=1,\dots,n+p-2} \sum_{j=1}^{n+p-2} \left| \int_0^1 N_{j+1,p}^{\mathbb{Q}_\mu}(x)\, (N_{i+1,p}^{\mathbb{Q}_\mu})'(x)\,\mathrm{d}x \right| \\
&= \max_{i=1,\dots,n+p-2} \sum_{j=1}^{n+p-2} \left| \int_0^1 N_{j+1,p}^{\mathbb{Q}_\mu}(x)\left(\delta_{i+1,p-1}^{\mathbb{Q}_\mu} N_{i+1,p-1}^{\mathbb{Q}_\mu}(x) - \delta_{i+2,p-1}^{\mathbb{Q}_\mu} N_{i+2,p-1}^{\mathbb{Q}_\mu}(x)\right)\mathrm{d}x \right| \\
&\leq \max_{i=1,\dots,n+p-2} \sum_{j=1}^{n+p-2} \int_0^1 N_{j+1,p}^{\mathbb{Q}_\mu}(x)\left(\delta_{i+1,p-1}^{\mathbb{Q}_\mu} N_{i+1,p-1}^{\mathbb{Q}_\mu}(x) + \delta_{i+2,p-1}^{\mathbb{Q}_\mu} N_{i+2,p-1}^{\mathbb{Q}_\mu}(x)\right)\mathrm{d}x.
\end{aligned}$$

Using the partition of unity property of GB-splines, we deduce

$$\begin{aligned}
&\sum_{j=1}^{n+p-2} \int_0^1 N_{j+1,p}^{\mathbb{Q}_\mu}(x)\delta_{i+1,p-1}^{\mathbb{Q}_\mu} N_{i+1,p-1}^{\mathbb{Q}_\mu}(x)\,\mathrm{d}x \\
&\quad = \int_0^1 \left(\sum_{j=1}^{n+p-2} N_{j+1,p}^{\mathbb{Q}_\mu}(x)\right)\delta_{i+1,p-1}^{\mathbb{Q}_\mu} N_{i+1,p-1}^{\mathbb{Q}_\mu}(x)\,\mathrm{d}x \leq \int_0^1 \delta_{i+1,p-1}^{\mathbb{Q}_\mu} N_{i+1,p-1}^{\mathbb{Q}_\mu}(x)\,\mathrm{d}x = 1.
\end{aligned}$$

Moreover, by repeating the argument for the other term, we get $\|H_{n,p}^{\mathbb{Q}_\mu}\|_\infty \leq 2$. Finally,

$$\begin{aligned}
\left\|nK_{n,p}^{\mathbb{Q}_\mu}\right\|_\infty &= \max_{i=1,\dots,n+p-2} \sum_{j=1}^{n+p-2} \left| \int_0^1 \left(N_{j+1,p}^{\mathbb{Q}_\mu}\right)'(x) \left(N_{i+1,p}^{\mathbb{Q}_\mu}\right)'(x)\,\mathrm{d}x \right| \\
&= \max_{i=1,\dots,n+p-2} \sum_{j=1}^{n+p-2} \left| \int_0^1 \left(\delta_{j+1,p-1}^{\mathbb{Q}_\mu} N_{j+1,p-1}^{\mathbb{Q}_\mu}(x) - \delta_{j+2,p-1}^{\mathbb{Q}_\mu} N_{j+2,p-1}^{\mathbb{Q}_\mu}(x)\right)\right. \\
&\qquad \left. \cdot\left(\delta_{i+1,p-1}^{\mathbb{Q}_\mu} N_{i+1,p-1}^{\mathbb{Q}_\mu}(x) - \delta_{i+2,p-1}^{\mathbb{Q}_\mu} N_{i+2,p-1}^{\mathbb{Q}_\mu}(x)\right)\mathrm{d}x \right|.
\end{aligned}$$

Since the GB-splines of degree 1 are bounded as

$$N_{j,1}^{\mathbb{H}_\mu}(t) \leq 1, \quad N_{j,1}^{\mathbb{T}_\mu}(t) \leq \begin{cases} 1, & \text{if } \mu/n \in (0,\pi/2], \\ 1/\sin(\mu/n), & \text{if } \mu/n \in (\pi/2,\pi), \end{cases}$$

and using again the partition of unity property of GB-splines (for degree ≥ 2), we deduce that

$$\begin{aligned} &\sum_{j=1}^{n+p-2} \int_0^1 \delta_{j+1,p-1}^{\mathbb{Q}_\mu} N_{j+1,p-1}^{\mathbb{Q}_\mu}(x) \delta_{i+1,p-1}^{\mathbb{Q}_\mu} N_{i+1,p-1}^{\mathbb{Q}_\mu}(x)\,\mathrm{d}x \\ &\quad = \int_0^1 \left(\sum_{j=1}^{n+p-2} \delta_{j+1,p-1}^{\mathbb{Q}_\mu} N_{j+1,p-1}^{\mathbb{Q}_\mu}(x) \right) \delta_{i+1,p-1}^{\mathbb{Q}_\mu} N_{i+1,p-1}^{\mathbb{Q}_\mu}(x)\,\mathrm{d}x \\ &\quad \leq \breve{C}_{p,\alpha} \max_{j=1,\ldots,n+p-2} \delta_{j+1,p-1}^{\mathbb{Q}_\mu} \int_0^1 \delta_{i+1,p-1}^{\mathbb{Q}_\mu} N_{i+1,p-1}^{\mathbb{Q}_\mu}(x)\,\mathrm{d}x = \breve{C}_{p,\alpha} \max_{j=1,\ldots,n+p-2} \delta_{j+1,p-1}^{\mathbb{Q}_\mu}, \end{aligned}$$

where $\breve{C}_{p,\alpha}$ is a constant independent of n. We can use a similar reasoning for the other three terms in the expression of $\|nK_{n,p}^{\mathbb{Q}_\mu}\|_\infty$. It remains to prove that

$$\max_{j=1,\ldots,n+p-2} \delta_{j+1,p-1}^{\mathbb{Q}_\mu} \leq \widetilde{C}_{p,\alpha}\, n,$$

for some constant $\widetilde{C}_{p,\alpha}$ independent of n. We first observe that for $i = p,\ldots,n$,

$$\frac{1}{\delta_{i,p-1}^{\mathbb{Q}_\mu}} = \int_0^1 N_{i,p-1}^{\mathbb{Q}_\mu}(s)\,\mathrm{d}s = \int_0^1 \phi_{p-1}^{\mathbb{Q}_{\mu/n}}(ns-i+p)\mathrm{d}s = \frac{1}{n}\int_0^p \phi_{p-1}^{\mathbb{Q}_{\mu/n}}(z)\mathrm{d}z = \frac{1}{n}.$$

For $i \in I := \{2,\ldots,p-1,n+1,\ldots,n+p-1\}$, we address the nested and non-nested cases separately.

- *Case $\mu = \alpha$:* $\delta_{i,p-1}^{\mathbb{Q}_\alpha} = k_{i,p-1}^{\alpha,n} n$, where $k_{i,p-1}^{\alpha,n}$ is dependent on n but can be bounded above by a constant independent of n. Indeed, because of its convergence to the polynomial setting and the explicit B-spline integral formula (see, e.g., [14]) we have

  $$\lim_{n\to\infty} k_{i,p-1}^{\alpha,n} = \lim_{n\to\infty} \frac{p}{n(t_{i+p}-t_i)} \leq p.$$

  This implies the existence of an integer n_0 for which $k_{i,p-1}^{\alpha,n} \leq 2p$ for every $n > n_0$.
- *Case $\mu = n\alpha$:* $\delta_{i,p-1}^{\mathbb{Q}_{n\alpha}} = k_{i,p-1}^{\alpha,n} n$, where $k_{i,p-1}^{\alpha,n}$ is independent of n for $n \geq p-1$. This holds because the integrals $\int_0^1 N_{i,p-1}^{\mathbb{Q}_{n\alpha}}(s)\,\mathrm{d}s$ are proportional to the support of $N_{i,p-1}^{\mathbb{Q}_{n\alpha}}(s)$, and so to $1/n$. More precisely, fixing $1 < i < p$, it can be proved by induction that the GB-spline $N_{i,p-1}^{\mathbb{Q}_{n_1\alpha}}$ defined over the knot set (10) with n_1 intervals and the GB-spline $N_{i,p-1}^{\mathbb{Q}_{n_2\alpha}}$ defined over the knot set (10) with n_2 intervals are related by

  $$N_{i,p-1}^{\mathbb{Q}_{n_1\alpha}}(n_2 x) = N_{i,p-1}^{\mathbb{Q}_{n_2\alpha}}(n_1 x).$$

  By taking into account their local supports, we get

  $$\frac{n_1}{\delta_{i,p-1}^{\mathbb{Q}_{n_1\alpha}}} = n_1 \int_0^{i/n_1} N_{i,p-1}^{\mathbb{Q}_{n_1\alpha}}(s)\,\mathrm{d}s = n_2 \int_0^{i/n_2} N_{i,p-1}^{\mathbb{Q}_{n_2\alpha}}(s)\,\mathrm{d}s = \frac{n_2}{\delta_{i,p-1}^{\mathbb{Q}_{n_2\alpha}}}.$$

□

We are now ready to determine the spectral distribution of the sequence of (normalized) matrices $\frac{1}{n}A_{n,p}^{\mathbb{Q}_\mu}$, $\mathbb{Q} = \mathbb{H}, \mathbb{T}$, both for the nested and non-nested case. We will first address the nested case in Section 4.2 and then the non-nested case in Section 4.3.

4.2 Spectral distribution: sequences of nested spaces

In this subsection we focus on the spectral distribution of the sequence of matrices

$$\frac{1}{n}A_{n,p}^{\mathbb{Q}_\alpha} = K_{n,p}^{\mathbb{Q}_\alpha} + \frac{\beta}{n}H_{n,p}^{\mathbb{Q}_\alpha} + \frac{\gamma}{n^2}M_{n,p}^{\mathbb{Q}_\alpha}, \quad \mathbb{Q} = \mathbb{H}, \mathbb{T}, \tag{69}$$

where α is a real positive parameter not depending on n. We first show that both sequences $\{K_{n,p}^{\mathbb{Q}_\alpha}\}$ and $\{B_{n,p}^{\mathbb{Q}_\alpha}\}$, see (67), share the same spectral distribution.

Lemma 8 *Let α be a real parameter independent of n. For $p \geq 2$, it holds*

$$\{B_{n,p}^{\mathbb{Q}_\alpha}\} \sim_\lambda f_p, \quad \{K_{n,p}^{\mathbb{Q}_\alpha}\} \sim_\lambda f_p, \quad \mathbb{Q} = \mathbb{H}, \mathbb{T}.$$

Moreover, both sequences are strongly clustered at $[0, M_{f_p}]$.

Proof We first prove the spectral distribution of $\{B_{n,p}^{\mathbb{Q}_\alpha}\}$. By Lemma 6 we have

$$B_{n,p}^{\mathbb{Q}_\alpha} = T_{n+p-2}\left(f_p^{\mathbb{Q}_{\alpha/n}}\right) = T_{n+p-2}(f_p) + T_{n+p-2}\left(f_p^{\mathbb{Q}_{\alpha/n}} - f_p\right),$$

and we apply Theorem 1, with

$$Z_n := B_{n,p}^{\mathbb{Q}_\alpha}, \quad X_n := T_{n+p-2}(f_p), \quad Y_n := T_{n+p-2}\left(f_p^{\mathbb{Q}_{\alpha/n}} - f_p\right).$$

From Theorem 3 it follows

$$\|T_{n+p-2}(f_p)\| \leq \|f_p\|_{L_\infty([-\pi,\pi])}, \tag{70}$$

and

$$\left\|T_{n+p-2}\left(f_p^{\mathbb{Q}_{\alpha/n}} - f_p\right)\right\|_1 \leq (n+p-2)\left\|f_p^{\mathbb{Q}_{\alpha/n}} - f_p\right\|_{L_1([-\pi,\pi])}. \tag{71}$$

The matrix X_n is Hermitian by construction, and so Theorem 2 implies that $\{X_n\} \sim_\lambda f_p$ and $\{X_n\}$ is strongly clustered at $[0, M_{f_p}]$, which is the essential range of f_p. From (70) and (58) we obtain that $\|X_n\|$ can be bounded by a constant independent of n. Moreover, by combining the result in Lemma 5 with (71) we see that $\|Y_n\|_1$ can be bounded by a constant independent of n. Therefore, all the hypotheses of Theorem 1 are satisfied, and we have that $\{B_{n,p}^{\mathbb{Q}_\alpha}\} \sim_\lambda f_p$ and $\{B_{n,p}^{\mathbb{Q}_\alpha}\}$ is strongly clustered at $[0, M_{f_p}]$.

To prove the spectral distribution of $\{K_{n,p}^{\mathbb{Q}_\alpha}\}$, we consider again Theorem 1, but now with

$$Z_n := K_{n,p}^{\mathbb{Q}_\alpha}, \quad X_n := B_{n,p}^{\mathbb{Q}_\alpha}, \quad Y_n := R_{n,p}^{\mathbb{Q}_\alpha}.$$

Recalling that $K_{n,p}^{\mathbb{Q}_\alpha}$ is symmetric and using Lemma 6 and Theorem 3, we have

$$\|K_{n,p}^{\mathbb{Q}_\alpha}\| \leq \|K_{n,p}^{\mathbb{Q}_\alpha}\|_\infty, \quad \|B_{n,p}^{\mathbb{Q}_\alpha}\| \leq \left\|f_p^{\mathbb{Q}_{\alpha/n}}\right\|_{L_\infty([-\pi,\pi])}, \tag{72}$$

which can be both bounded independently of n, thanks to the upper bounds in Lemma 7 and Lemma 3, respectively. Moreover, from (67) and (68) we obtain

$$\|R_{n,p}^{\mathbb{Q}_\alpha}\|_1 \leq 2(2p-1)\|R_{n,p}^{\mathbb{Q}_\alpha}\|, \quad \|R_{n,p}^{\mathbb{Q}_\alpha}\| = \|K_{n,p}^{\mathbb{Q}_\alpha} - B_{n,p}^{\mathbb{Q}_\alpha}\| \leq \|B_{n,p}^{\mathbb{Q}_\alpha}\| + \|K_{n,p}^{\mathbb{Q}_\alpha}\|,$$

which can also be bounded independently of n, thanks to (72). Therefore, both $\|X_n\|$ and $\|Y_n\|_1$ can be bounded by a constant independent of n, and all the hypotheses of Theorem 1 are satisfied. This completes the proof. □

Finally, the next theorem states the spectral distribution result for $\{\frac{1}{n}A^{\mathbb{Q}_\alpha}_{n,p}\}$.

Theorem 5 *Let α be a real parameter independent of n. For $p \geq 2$ and $\mathbb{Q} = \mathbb{H}, \mathbb{T}$, the sequence of matrices $\{\frac{1}{n}A^{\mathbb{Q}_\alpha}_{n,p}\}$ is distributed like the function f_p given in (54) in the sense of the eigenvalues and it is strongly clustered at $[0, M_{f_p}]$.*

Proof According to the matrix decomposition in (69), we consider Theorem 1 with

$$Z_n := \frac{1}{n}A^{\mathbb{Q}_\alpha}_{n,p}, \quad X_n := K^{\mathbb{Q}_\alpha}_{n,p}, \quad Y_n := \frac{\beta}{n}H^{\mathbb{Q}_\alpha}_{n,p} + \frac{\gamma}{n^2}M^{\mathbb{Q}_\alpha}_{n,p}.$$

From Lemma 8 and its proof we know that $\{K^{\mathbb{Q}_\alpha}_{n,p}\} \sim_\lambda f_p$, $\{K^{\mathbb{Q}_\alpha}_{n,p}\}$ is strongly clustered at $[0, M_{f_p}]$ and $\|K^{\mathbb{Q}_\alpha}_{n,p}\|$ can be bounded independently of n. Moreover, $H^{\mathbb{Q}_\alpha}_{n,p}$ and $M^{\mathbb{Q}_\alpha}_{n,p}$ are normal matrices, so

$$\begin{aligned}
\|Y_n\|_1 &\leq \frac{|\beta|}{n}\|H^{\mathbb{Q}_\alpha}_{n,p}\|_1 + \frac{\gamma}{n^2}\|M^{\mathbb{Q}_\alpha}_{n,p}\|_1 \\
&\leq |\beta|\frac{n+p-2}{n}\|H^{\mathbb{Q}_\alpha}_{n,p}\| + \gamma\frac{n+p-2}{n^2}\|M^{\mathbb{Q}_\alpha}_{n,p}\| \\
&\leq |\beta|\frac{n+p-2}{n}\|H^{\mathbb{Q}_\alpha}_{n,p}\|_\infty + \gamma\frac{n+p-2}{n^2}\|M^{\mathbb{Q}_\alpha}_{n,p}\|_\infty,
\end{aligned}$$

which can be bounded independently of n, thanks to the upper bounds in Lemma 7. So all the hypotheses of Theorem 1 are satisfied and the result follows. □

Remark 9 From (57)–(58) it follows that the symbol $f_p(\theta)$ of the sequence $\{\frac{1}{n}A^{\mathbb{Q}_\alpha}_{n,p}\}$ has a unique zero at $\theta = 0$. Moreover, from (59) we see that $f_p(\pi)$ converges exponentially to zero with respect to p, so $f_p(\pi)$ is very small for large p and will behave numerically like a zero.

Remark 10 As pointed out in [9, 10] for the (polynomial) B-spline case, the 'numerical zero' of f_p at $\theta = \pi$ (for larger values of p) negatively affects the convergence rate of standard multigrid methods. This leads to an unsatisfactory behavior of standard multigrid methods, even for moderate values of p and not only for unrealistically large values of p. For instance, looking at [9, Table 4], we see that in the Galerkin formulation with B-splines of degree p, the convergence rate of standard multigrid methods (using Richardson smoothing) is already very slow for $p \geq 6$, and a similar – even worse – phenomenon is observed in higher dimensionality $d > 1$. We expect that the same unsatisfactory multigrid behavior also occurs in the hyperbolic/trigonometric GB-spline case.

Remark 11 The intrinsic difficulty for larger values of p, described in Remark 10, can be addressed by following the multi-iterative idea from [26]. Indeed, in [9] and [10], a standard multigrid method was successfully combined with a smoother of preconditioned Krylov type (namely PCG and PGMRES, respectively), where the preconditioner was suggested by the symbol. This results in a robust and optimal multi-iterative multigrid solver. We expect that a similar technique can also be used in the hyperbolic/trigonometric GB-spline case.

4.3 Spectral distribution: sequences of non-nested spaces

In this subsection we focus on the spectral distribution of the sequence of matrices

$$\frac{1}{n}A_{n,p}^{\mathbb{Q}_{n\alpha}} = K_{n,p}^{\mathbb{Q}_{n\alpha}} + \frac{\beta}{n}H_{n,p}^{\mathbb{Q}_{n\alpha}} + \frac{\gamma}{n^2}M_{n,p}^{\mathbb{Q}_{n\alpha}}, \quad \mathbb{Q} = \mathbb{H}, \mathbb{T}, \tag{73}$$

where α is a real positive parameter not depending on n. The next lemma provides the spectral distribution of the sequences $\{K_{n,p}^{\mathbb{Q}_{n\alpha}}\}$ and $\{B_{n,p}^{\mathbb{Q}_{n\alpha}}\}$.

Lemma 9 *Let α be a real parameter independent of n, For $p \geq 2$, it holds*

$$\{B_{n,p}^{\mathbb{Q}_{n\alpha}}\} \sim_\lambda f_p^{\mathbb{Q}_\alpha}, \quad \{K_{n,p}^{\mathbb{Q}_{n\alpha}}\} \sim_\lambda f_p^{\mathbb{Q}_\alpha}, \quad \mathbb{Q} = \mathbb{H}, \mathbb{T}.$$

Moreover, both sequences are strongly clustered at $[0, M_{f_p^{\mathbb{Q}_\alpha}}]$.

Proof From Lemma 6 we know

$$B_{n,p}^{\mathbb{Q}_{n\alpha}} = T_{n+p-2}(f_p^{\mathbb{Q}_\alpha}).$$

Therefore, Theorem 2 implies that $\{B_{n,p}^{\mathbb{Q}_{n\alpha}}\} \sim_\lambda f_p^{\mathbb{Q}_\alpha}$ and $\{B_{n,p}^{\mathbb{Q}_{n\alpha}}\}$ is strongly clustered at $[0, M_{f_p^{\mathbb{Q}_\alpha}}]$. The spectral distribution of $\{K_{n,p}^{\mathbb{Q}_{n\alpha}}\}$ can be shown by following the same line of arguments as in the proof of Lemma 8. □

The spectral distribution of the sequence of matrices (73) can be obtained with the same arguments as for Theorem 5. The results are stated in the next theorem.

Theorem 6 *Let α be a real parameter independent of n. For $p \geq 2$ and $\mathbb{Q} = \mathbb{H}, \mathbb{T}$, the sequence of matrices $\{\frac{1}{n}A_{n,p}^{\mathbb{Q}_{n\alpha}}\}$ is distributed like the function $f_p^{\mathbb{Q}_\alpha}$ given in (55)–(56) in the sense of the eigenvalues and it is strongly clustered at* $[0, M_{f_p^{\mathbb{Q}_\alpha}}]$.

Remark 12 From Lemma 3 we know that the symbol $f_p^{\mathbb{Q}_\alpha}(\theta)$ of the sequence $\{\frac{1}{n}A_{n,p}^{\mathbb{Q}_{n\alpha}}\}$ has a (theoretical) zero at $\theta = 0$, and from Lemma 4 it follows that this symbol has a 'numerical zero' at $\theta = \pi$ for large p, see also Remark 9. We expect that the same unsatisfactory multigrid behavior described in Remark 10 also occurs in this hyperbolic/trigonometric GB-spline case, with a possible multi-iterative remedy as suggested in Remark 11.

4.4 Spectral approximation for finite dimensional matrices

The spectral analysis in Section 4.2 shows that the stiffness matrices corresponding to a Galerkin discretization based on a sequence of nested generalized hyperbolic/trigonometric spaces of degree p (with fixed phase parameter α) have the same (asymptotic) spectral distribution as the matrices resulting from a Galerkin discretization based on classical polynomial spline spaces of the same degree. This distribution is described by the function f_p. As mentioned in Remark 3, this means that the spectrum of these matrices behaves like a uniform sampling of f_p when their size increases.

Due to (61), however, it is reasonable to expect that the function $f_p^{\mathbb{Q}_{\alpha/n}}$ provides a more accurate description of the spectrum of $K_{n,p}^{\mathbb{Q}_\alpha}$, and so of $\frac{1}{n}A_{n,p}^{\mathbb{Q}_\alpha}$ (see Theorem 5), for finite (small) values of n. This is actually the case as illustrated in the following examples.

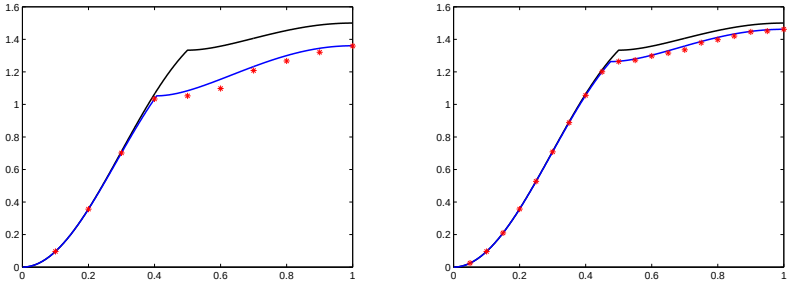

Fig. 2 Sorted eigenvalues of $K_{n,p}^{\mathbb{T}_\alpha}$ with $\alpha = 4\pi$, $p = 2$ (red $*$) compared with sorted uniform samples of $f_p^{\mathbb{T}_{\alpha/n}}$ (blue line) and f_p (black line). Left: $n = 10$. Right: $n = 20$.

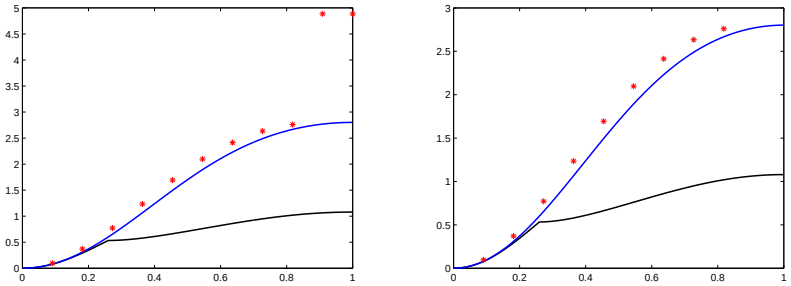

Fig. 3 Left: sorted eigenvalues of $K_{n,p}^{\mathbb{H}_\alpha}$ with $\alpha = 100$, $p = 3$ and $n = 10$ (red $*$) compared with sorted uniform samples of $f_p^{\mathbb{H}_{\alpha/n}}$ (blue line) and f_p (black line). Right: a magnified version.

Figures 2–4 illustrate the eigenvalues of the matrix $K_{n,p}^{\mathbb{Q}_\alpha}$ for different values of the parameters p and n, for hyperbolic and trigonometric spline spaces with various choices of the phase parameter α. The values of the parameters in Figure 3 are inspired by those in [24, Example 3], whereas the parameters considered in Figure 4 are taken from [25, Section 4.2.2]. We compared the eigenvalues of $K_{n,p}^{\mathbb{Q}_\alpha}$ with the functions f_p and $f_p^{\mathbb{Q}_{\alpha/n}}$ over $(0,\pi)$. More precisely, we considered equispaced samples of f_p and $f_p^{\mathbb{Q}_{\alpha/n}}$ at the points

$$\left\{\frac{k\pi}{m+1} : k = 1,\dots,m\right\}, \quad m = 1000.$$

To make a fair comparison we sorted the three sets of values. Except for possibly few outliers, we see an extremely good match between the function $f_p^{\mathbb{Q}_{\alpha/n}}$ and the spectrum. Note that the presence of two outliers for $p = 3,4$ (clearly depicted in Figures 3–4 (left)) is in a complete agreement with the fact that the sequence of matrices $\{K_{n,p}^{\mathbb{Q}_\alpha}\}$ is strongly clustered at $[0, M_{f_p}]$, see Definition 3 and Theorem 5.

We may conclude that the analysis of the symbols $f_p^{\mathbb{Q}_{\alpha/n}}$ presented in Section 3.3 is of interest not only to describe the spectral distribution of the matrices arising from Galerkin discretizations based on non-nested spaces, but also because they provide a precise description of the spectrum of the matrices obtained in the case of nested spaces for finite (small) values of n.

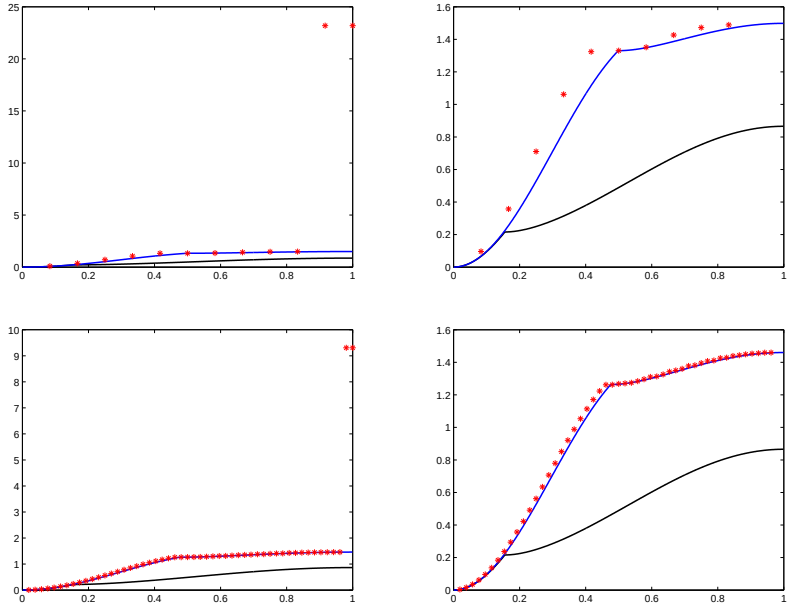

Fig. 4 Left: sorted eigenvalues of $K_{n,p}^{\mathbb{H}_\alpha}$ with $\alpha = 1000$, $p = 4$ (red $*$) compared with sorted uniform samples of $f_p^{\mathbb{H}_{\alpha/n}}$ (blue line) and f_p (black line). Right: a magnified version. Top: $n = 10$. Bottom: $n = 50$.

5 Spectral analysis in case of our eigenvalue problem

In this section we address the eigenvalue problem (8). Due to the structure of the problem, it is natural to consider an approximation based on trigonometric GB-splines. So, we are interested in the eigenvalues of the matrices in (21) where the Galerkin discretization is based on trigonometric GB-splines, i.e.,

$$L_{n,p}^{\mathbb{T}_\mu} := n^2 (M_{n,p}^{\mathbb{T}_\mu})^{-1} K_{n,p}^{\mathbb{T}_\mu}. \tag{74}$$

As mentioned in Section 2.1.2, the $N := n + p - 2$ eigenvalues of the matrix (74) are used to approximate the first N eigenvalues ω_k in (9) associated with the eigenfunctions

$$u_k(x) = \sin(\omega_k x), \quad k = 1, \ldots, N.$$

This means that higher frequencies are addressed as the dimension of the discretization space $\mathcal{W}_{n,p}^{\mathbb{T}_\mu}$ increases. As a consequence, it is natural to consider trigonometric spline spaces whose phase increases linearly with respect to their dimension. This motivates the interest in Galerkin discretizations based on the space $\mathcal{W}_{n,p}^{\mathbb{T}_{n\alpha}}$ where α is a fixed real parameter belonging to $(0, \pi)$. Equivalently, this means that we will consider generalized spline spaces over the knot set (10) with sections in

$$\langle 1, x, \ldots, x^{p-2}, \cos(n\alpha x), \sin(n\alpha x) \rangle.$$

Note that the assumption $n\alpha(t_{i+1} - t_i) < \pi$ is satisfied because $t_{i+1} - t_i \leq \frac{1}{n}$.

5.1 Spectral distribution of $\{n^{-2}L_{n,p}^{\mathbb{T}_{n\alpha}}\}$

We now investigate the spectral distribution of the sequence $\{n^{-2}L_{n,p}^{\mathbb{T}_{n\alpha}}\}$. To this end, we first look at the spectral distribution of the sequence $\{M_{n,p}^{\mathbb{T}_{n\alpha}}\}$, for which we can follow the same strategy as for the sequence $\{K_{n,p}^{\mathbb{Q}_{n\alpha}}\}$ considered in Sections 4.1 and 4.3. We decompose the matrix $M_{n,p}^{\mathbb{T}_{n\alpha}}$ into

$$M_{n,p}^{\mathbb{T}_{n\alpha}} = C_{n,p}^{\mathbb{T}_{n\alpha}} + S_{n,p}^{\mathbb{T}_{n\alpha}}, \tag{75}$$

where $C_{n,p}^{\mathbb{T}_{n\alpha}}$ is the symmetric $(2p+1)$-band Toeplitz matrix whose generic central row is given by (66). The matrix $S_{n,p}^{\mathbb{T}_{n\alpha}} := M_{n,p}^{\mathbb{T}_{n\alpha}} - C_{n,p}^{\mathbb{T}_{n\alpha}}$ is a low-rank correction term analogous to $R_{n,p}^{\mathbb{T}_{n\alpha}}$ and so

$$\operatorname{rank}(S_{n,p}^{\mathbb{T}_{n\alpha}}) \leq 2(2p-1). \tag{76}$$

The following spectral properties of $\{C_{n,p}^{\mathbb{T}_{n\alpha}}\}$ and $\{M_{n,p}^{\mathbb{T}_{n\alpha}}\}$ can be obtained by using the same line of arguments as for Lemmas 6 and 9. We omit the proofs for the sake of brevity.

Lemma 10 *Let α be a real parameter in $(0,\pi)$ independent of n. For $p \geq 1$ and $n \geq 3p+1$, it holds*

$$C_{n,p}^{\mathbb{T}_{n\alpha}} = T_{n+p-2}(h_p^{\mathbb{T}_\alpha}) \quad \textit{with} \quad \sigma(C_{n,p}^{\mathbb{T}_{n\alpha}}) \subset \left(m_{h_p^{\mathbb{T}_\alpha}}, 1\right).$$

Lemma 11 *Let α be a real parameter in $(0,\pi)$ independent of n. For $p \geq 1$, it holds*

$$\{C_{n,p}^{\mathbb{T}_{n\alpha}}\} \sim_\lambda h_p^{\mathbb{T}_\alpha}, \quad \{M_{n,p}^{\mathbb{T}_{n\alpha}}\} \sim_\lambda h_p^{\mathbb{T}_\alpha}.$$

Moreover, both sequences are strongly clustered at $[m_{h_p^{\mathbb{T}_\alpha}}, 1]$.

The spectral distribution of the sequence $\{n^{-2}L_{n,p}^{\mathbb{T}_{n\alpha}}\}$ can be derived by exploiting the powerful theory of GLT sequences [16,29]. A GLT sequence $\{X_n\}$ is a specific sequence of matrices with $\text{size}(X_n) \to \infty$, equipped with a function κ (the symbol of the sequence), see [29, Definition 1.5]. GLT sequences form an algebra and possess several remarkable properties [16,29]:

- If $\{X_n\}$ is a GLT sequence of Hermitian matrices with symbol κ, then $\{X_n\} \sim_\lambda \kappa$.
- For every $f \in L^1([-\pi,\pi])$, the Toeplitz sequence $\{T_n(f)\}$ is a GLT sequence with symbol f.
- If $\{X_n\}$ is a GLT sequence with symbol κ and $\lim_{n\to\infty} \|E_n\| = \lim_{n\to\infty} \text{rank}(R_n)/\text{size}(X_n) = 0$, then $\{X_n + E_n + R_n\}$ is a GLT sequence with symbol κ.
- If $\{X_n^{(i)}\}$ are GLT sequences with symbols κ_i, for $i = 1,\dots,r$, then $\{X_n^{(1)} \cdots X_n^{(r)}\}$ is a GLT sequence with symbol $\kappa_1 \cdots \kappa_r$.
- If $\{X_n\}$ is a GLT sequence of invertible matrices with symbol κ and $\kappa \neq 0$ a.e., then $\{X_n^{-1}\}$ is a GLT sequence with symbol κ^{-1}.
- If $\{X_n\}$ is a GLT sequence of Hermitian matrices with symbol κ, then $\{g(X_n)\}$ is a GLT sequence with symbol $g(\kappa)$ for all continuous functions $g : \mathbb{R} \to \mathbb{R}$.

From (67), (75) and from Lemmas 6, 10 it follows that $K_{n,p}^{\mathbb{T}_{n\alpha}}$ and $M_{n,p}^{\mathbb{T}_{n\alpha}}$ are Hermitian perturbations of the Hermitian Toeplitz matrices $T_{n+p-2}(f_p^{\mathbb{T}_\alpha})$ and $T_{n+p-2}(h_p^{\mathbb{T}_\alpha})$, respectively. Moreover, from (68) and (76) we see that the rank of the perturbation matrices $R_{n,p}^{\mathbb{T}_{n\alpha}}$ and $S_{n,p}^{\mathbb{T}_{n\alpha}}$ is bounded by a constant independent of n. Therefore, $\{K_{n,p}^{\mathbb{T}_{n\alpha}}\}$ and $\{M_{n,p}^{\mathbb{T}_{n\alpha}}\}$ are simple instances of GLT sequences with symbols given by $f_p^{\mathbb{T}_\alpha}$ and $h_p^{\mathbb{T}_\alpha}$, respectively. Finally, by (48) we have $h_p^{\mathbb{T}_\alpha} > 0$, and $(M_{n,p}^{\mathbb{T}_{n\alpha}})^{-1}K_{n,p}^{\mathbb{T}_{n\alpha}}$ is similar to the Hermitian matrix $(M_{n,p}^{\mathbb{T}_{n\alpha}})^{-1/2}K_{n,p}^{\mathbb{T}_{n\alpha}}(M_{n,p}^{\mathbb{T}_{n\alpha}})^{-1/2}$. This leads to the following important result, see also [13].

Theorem 7 *Let α be a given real parameter in $(0,\pi)$. Then the sequence of matrices $\{n^{-2}L_{n,p}^{\mathbb{T}_{n\alpha}}\} := \{(M_{n,p}^{\mathbb{T}_{n\alpha}})^{-1}K_{n,p}^{\mathbb{T}_{n\alpha}}\}$ is distributed like the function*

$$(h_p^{\mathbb{T}_\alpha})^{-1} f_p^{\mathbb{T}_\alpha} \tag{77}$$

in the sense of the eigenvalues.

Thanks to this theorem, for large n, the eigenvalues of the matrix $n^{-2}L_{n,p}^{\mathbb{T}_{n\alpha}}$ can be approximately seen as a uniform sampling of the even function in (77).

Remark 13 For the sake of simplicity, we just formulated and proved the above results in case of a sequence of trigonometric spline spaces $\mathcal{W}_{n,p}^{\mathbb{T}_{n\alpha}}$, but similar results hold in a more general setting. In particular, using the same notation as in Section 4, we have for $\mathbb{Q} = \mathbb{H}, \mathbb{T}$,

$$\{M_{n,p}^{\mathbb{Q}_\mu}\} \sim_\lambda \begin{cases} h_p^{\mathbb{Q}_\alpha}, & \text{if } \mu = n\alpha, \\ h_p, & \text{if } \mu = \alpha, \end{cases}$$

and

$$\{n^{-2}L_{n,p}^{\mathbb{Q}_\mu}\} \sim_\lambda \begin{cases} (h_p^{\mathbb{Q}_\alpha})^{-1} f_p^{\mathbb{Q}_\alpha}, & \text{if } \mu = n\alpha, \\ (h_p)^{-1} f_p, & \text{if } \mu = \alpha. \end{cases}$$

This can be proved with similar arguments as used in this and the previous section.

5.2 Approximating eigenvalues by means of non-nested spaces

Let us denote by

$$(\omega_k^{\mathbb{T}_{n\alpha}})^2, \quad k = 1,\dots,n+p-2$$

the eigenvalues of the matrix $L_{n,p}^{\mathbb{T}_{n\alpha}}$, i.e., the computed approximations of the first $N := n + p - 2$ eigenvalues of (8). We assume they are sorted according to their modulus. A popular way to measure the accuracy of these approximations is given by the following relative error (see, e.g., [7,13,20]):

$$\frac{(\omega_k^{\mathbb{T}_{n\alpha}})^2 - (\omega_k)^2}{(\omega_k)^2} = \left(\frac{\omega_k^{\mathbb{T}_{n\alpha}}}{k\pi}\right)^2 - 1, \quad k = 1,\dots,N. \tag{78}$$

From Theorem 7 we know that $(\omega_k^{\mathbb{T}_{n\alpha}})^2$ can be approximately seen, for large n, as a uniform sampling of the function $n^2(h_p^{\mathbb{T}_\alpha})^{-1} f_p^{\mathbb{T}_\alpha}$. Let $\theta_k := k\pi/n$, we get

$$\left(\frac{\omega_k^{\mathbb{T}_{n\alpha}}}{k\pi}\right)^2 - 1 \simeq \frac{f_p^{\mathbb{T}_\alpha}(\theta_k)}{h_p^{\mathbb{T}_\alpha}(\theta_k)} \frac{n^2}{k^2\pi^2} - 1 = \frac{f_p^{\mathbb{T}_\alpha}(\theta_k)}{h_p^{\mathbb{T}_\alpha}(\theta_k)} \frac{1}{\theta_k^2} - 1, \quad k = 1,\dots,n.$$

Hence, the relative spectral error in (78) can be approximated by a uniform sampling over $(0,\pi)$ of the function

$$e_p^{\mathbb{T}_\alpha}(\theta) := \frac{f_p^{\mathbb{T}_\alpha}(\theta)}{h_p^{\mathbb{T}_\alpha}(\theta)} \frac{1}{\theta^2} - 1. \tag{79}$$

This function has the following properties.

Lemma 12 *Let $e_p^{\mathbb{T}_\alpha}$ be defined as in (79). Then*

$$e_p^{\mathbb{T}_\alpha}(\theta) \geq 0, \quad \theta \in (0,\pi), \quad p \geq 2, \tag{80}$$

and

$$\lim_{\theta\to 0} e_p^{\mathbb{T}_\alpha}(\theta) = 0, \quad p \geq 3, \tag{81}$$

$$\lim_{\theta\to \alpha} e_p^{\mathbb{T}_\alpha}(\theta) = 0, \quad p \geq 2. \tag{82}$$

Proof Since $h_p^{\mathbb{T}_\alpha}(\theta) > 0$, the inequality (80) is equivalent to

$$f_p^{\mathbb{T}_\alpha}(\theta) \geq h_p^{\mathbb{T}_\alpha}(\theta)\theta^2, \quad \theta \in (0,\pi), \quad p \geq 2.$$

Using (36) and (38) we obtain

$$\left|\widehat{\phi_p^{\mathbb{T}_\alpha}}(\theta + 2k\pi)\right|^2 = \left(\frac{2-2\cos(\theta)}{(\theta+2k\pi)^2}\right)^{p-1}\left(\frac{\alpha^2}{1-\cos(\alpha)}\right)^2\left(\frac{\cos(\alpha)-\cos(\theta)}{(\theta+2k\pi)^2-\alpha^2}\right)^2. \tag{83}$$

Then, from (50) and (47) we deduce

$$\begin{aligned} f_p^{\mathbb{T}_\alpha}(\theta) &= (2-2\cos(\theta))\sum_{k\in\mathbb{Z}}\left\|\widehat{\phi_{p-1}^{\mathbb{T}_\alpha}}(\theta+2k\pi)\right\|^2 = \sum_{k\in\mathbb{Z}}(\theta+2k\pi)^2\left\|\widehat{\phi_p^{\mathbb{T}_\alpha}}(\theta+2k\pi)\right\|^2 \\ &\geq \sum_{k\in\mathbb{Z}}\theta^2\left\|\widehat{\phi_p^{\mathbb{T}_\alpha}}(\theta+2k\pi)\right\|^2 = h_p^{\mathbb{T}_\alpha}(\theta)\theta^2. \end{aligned}$$

To prove (81), we recall that $h_p^{\mathbb{T}_\alpha}$ is continuous and $h_p^{\mathbb{T}_\alpha}(0) = 1$ for $p \geq 2$. Hence, we get

$$\lim_{\theta\to 0}\frac{f_p^{\mathbb{T}_\alpha}(\theta)}{h_p^{\mathbb{T}_\alpha}(\theta)}\frac{1}{\theta^2} = \lim_{\theta\to 0}\frac{h_{p-1}^{\mathbb{T}_\alpha}(\theta)}{h_p^{\mathbb{T}_\alpha}(\theta)}\frac{(2-2\cos(\theta))}{\theta^2} = 1, \quad p \geq 3.$$

Finally, to prove (82), we first note from (83) that

$$\left|\widehat{\phi_p^{\mathbb{T}_\alpha}}(\alpha+2k\pi)\right|^2 = 0, \quad k \neq 0.$$

Then, by taking into account the uniform convergence of the series in (47), we obtain

$$\lim_{\theta\to\alpha}\frac{f_p^{\mathbb{T}_\alpha}(\theta)}{h_p^{\mathbb{T}_\alpha}(\theta)}\frac{1}{\theta^2} = \lim_{\theta\to\alpha}\frac{\sum_{k\in\mathbb{Z}}(\theta+2k\pi)^2\left\|\widehat{\phi_p^{\mathbb{T}_\alpha}}(\theta+2k\pi)\right\|^2}{\theta^2\sum_{k\in\mathbb{Z}}\left\|\widehat{\phi_p^{\mathbb{T}_\alpha}}(\theta+2k\pi)\right\|^2} = \lim_{\theta\to\alpha}\frac{\theta^2\left\|\widehat{\phi_p^{\mathbb{T}_\alpha}}(\theta)\right\|^2}{\theta^2\left\|\widehat{\phi_p^{\mathbb{T}_\alpha}}(\theta)\right\|^2} = 1.$$

□

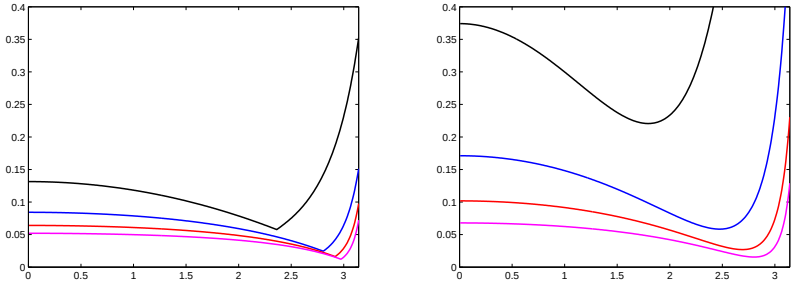

Fig. 5 From left to right: $\|e_p^{\mathbb{T}^\alpha}\|_{L_\infty([0,\pi])}$ and $\|e_p^{\mathbb{T}^\alpha}\|_{L_1([0,\pi])}$ as a function of the parameter α over $[0,\pi)$. Black: $p=2$, blue: $p=3$, red: $p=4$, magenta: $p=5$.

5.3 Numerical results

We now illustrate the performance of the Galerkin approximation using trigonometric spline spaces $\mathcal{W}_{n,p}^{\mathbb{T}_{n\alpha}}$ for the eigenvalue problem (8).

The selection of the parameter α is crucial in this approximation strategy. Two reasonable selection criteria are minimizing the L_∞-norm or the L_1-norm of the function $e_p^{\mathbb{T}^\alpha}$ in (79) which approximates the relative error given in (78). The graphs of these norms, as a function of the parameter $\alpha \in (0,\pi)$, are depicted in Figure 5 for different degrees.

In Figure 6 we plot the relative spectral error values

$$\left(\frac{k}{n}, \left(\frac{\omega_k^{\mathbb{T}_{n\alpha}}}{k\pi}\right)^2 - 1\right), \quad k = 1,\dots,n, \tag{84}$$

together with the graph of the function $e_p^{\mathbb{T}^\alpha}$ in (79). For comparison, we also plot the relative spectral error values and the graph of the corresponding function e_p in case of polynomial B-splines, i.e.,

$$e_p(\theta) := \frac{f_p(\theta)}{h_p(\theta)}\frac{1}{\theta^2} - 1. \tag{85}$$

Both the functions are rescaled over the interval $[0,1]$. The values of α are selected to (numerically) minimize $\|e_p^{\mathbb{T}^\alpha}\|_{L_\infty([0,\pi])}$. Figure 7 shows the analogous results in case the values of α are selected to (numerically) minimize $\|e_p^{\mathbb{T}^\alpha}\|_{L_1([0,\pi])}$. Finally, in Figure 8 we depict the results obtained by selecting α according to the heuristic suggestion[2] in [25, Eq. (18)].

We note that

- there is a very good match between the function $e_p^{\mathbb{T}^\alpha}$ in (79) obtained by our theoretical spectral analysis (blue line) and the computed relative error in (84) of the Galerkin approximation of the spectrum based on non-nested trigonometric spline spaces $\mathcal{W}_{n,p}^{\mathbb{T}_{n\alpha}}$ (red $*$);
- from Lemma 12 we know that $e_p^{\mathbb{T}^\alpha}(\theta)$ is non-negative and attains the value zero at $\theta = 0$ and $\theta = \alpha$; in addition, we observe in the figures that $e_p^{\mathbb{T}^\alpha}(\pi)$ is very close to zero;
- as explained in [13], the relative error of the Galerkin approximation of the spectrum based on polynomial spline spaces (black $\circ$) is accurately described by the function e_p in (85) which can be derived by a similar theoretical spectral analysis (black line);

[2] For polynomial B-splines, a degree p in Galerkin approximation corresponds to a degree $2p+1$ in collocation, see [11, Remark 3.2]. We have followed the same rule here.

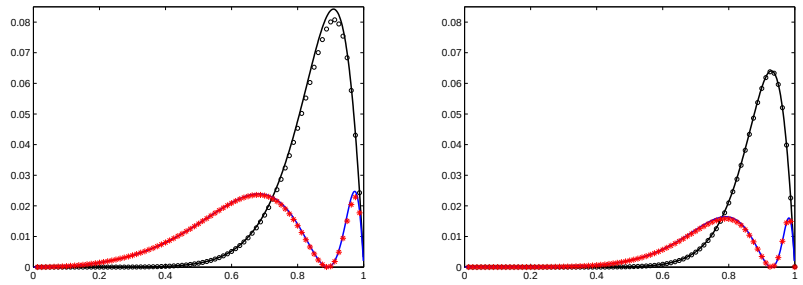

Fig. 6 Plot of the relative spectral error values in the trigonometric case (red $*$) and the polynomial case (black $\circ$) for $n = 80$, together with the scaled graphs of $e_p^{\mathbb{T}_\alpha}$ (blue line) and e_p (black line). The values of α are taken to (numerically) minimize $\|e_p^{\mathbb{T}_\alpha}\|_{L_\infty([0,\pi])}$. Left: $p = 3$, $\alpha = 2.80$. Right: $p = 4$, $\alpha = 2.92$.

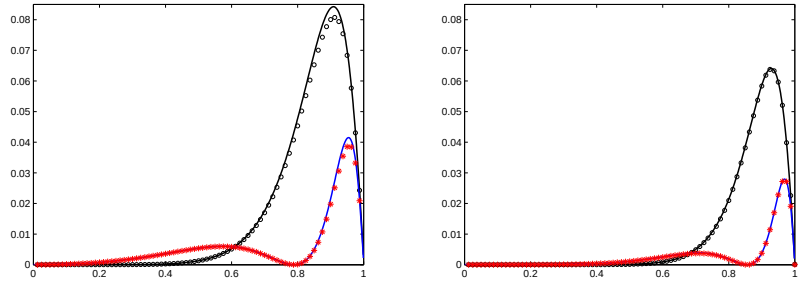

Fig. 7 Plot of the relative spectral error values in the trigonometric case (red $*$) and the polynomial case (black $\circ$) for $n = 80$, together with the scaled graphs of $e_p^{\mathbb{T}_\alpha}$ (blue line) and e_p (black line). The values of α are taken to (numerically) minimize $\|e_p^{\mathbb{T}_\alpha}\|_{L_1([0,\pi])}$. Left: $p = 3$, $\alpha = 2.48$. Right: $p = 4$, $\alpha = 2.69$.

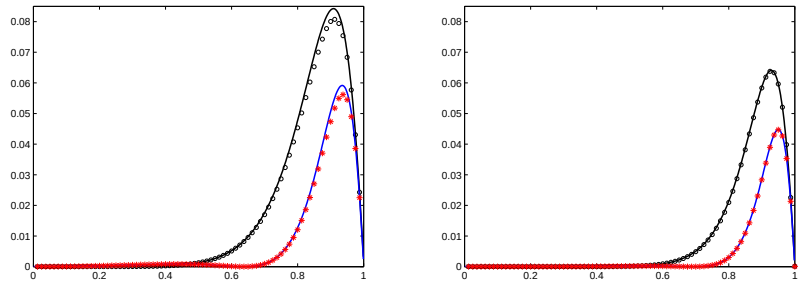

Fig. 8 Plot of the relative spectral error values in the trigonometric case (red $*$) and the polynomial case (black $\circ$) for $n = 80$, together with the scaled graphs of $e_p^{\mathbb{T}_\alpha}$ (blue line) and e_p (black line). Left: $p = 3$, $\alpha = \frac{7}{11}\pi$. Right: $p = 4$, $\alpha = \frac{9}{13}\pi$.

– since trigonometric GB-splines approach classical (polynomial) B-splines when the phase parameter approaches 0 (see Remark 1) and since the sequences $\{K_{n,p}^{\mathbb{Q}_\alpha}\}$, $\{M_{n,p}^{\mathbb{Q}_\alpha}\}$ are distributed like f_p, h_p respectively in the sense of eigenvalues, the relative error of the Galerkin approximation of the spectrum based on nested trigonometric spline spaces $\mathcal{W}_{n,p}^{\mathbb{T}_\alpha}$ is accurately described by the function e_p in (85). The corresponding plots are

omitted because they are indistinguishable from the polynomial case for the considered values of n; we also refer to [25] for analogous results in case of collocation methods.

As a consequence, the use of non-nested trigonometric spline spaces $\mathcal{W}_{n,p}^{\mathbb{T}_{n\alpha}}$ results in a more flexible approximation tool for the eigenvalue problem than the classical (polynomial) B-spline discretization and the discretization by means of nested trigonometric spline spaces $\mathcal{W}_{n,p}^{\mathbb{T}_{\alpha}}$. The minimization of the L_∞-norm or the L_1-norm can be valid criteria for the selection of the parameter α. Nevertheless, other alternative criteria can be more appropriate according to the demands of the user.

6 The multivariate setting

In this section we outline the extension of the spectral results given in Section 4 to the multi-dimensional version of the linear elliptic differential problem (1), i.e.,

$$\begin{cases} -\Delta u + \boldsymbol{\beta}\nabla u + \gamma u = \mathrm{f}, & \text{in } \Omega, \\ u = 0, & \text{on } \partial\Omega. \end{cases} \tag{86}$$

where $\Omega := (0,1)^d$, $\boldsymbol{\beta} := (\beta_1,\dots,\beta_d) \in \mathbb{R}^d$, $\gamma \geq 0$, $\mathrm{f} \in L_2(\Omega)$. The weak form of (86) consists in finding $u \in H_0^1(\Omega)$ such that

$$\int_\Omega (\nabla u)^T \nabla v + (\nabla u)^T \boldsymbol{\beta} v + \gamma u v = \int_\Omega \mathrm{f} v, \quad \forall v \in H_0^1(\Omega).$$

Following the Galerkin approach, we look for an approximation $u_{\mathcal{W}} = \sum_{j=1}^N u_j \varphi_j$ of u belonging to a finite dimensional approximation space $\mathcal{W} \subset H_0^1(\Omega)$ spanned by the basis $\{\varphi_1,\dots,\varphi_N\}$. This is equivalent to solving the linear system $A\mathbf{u} = \mathbf{f}$, where

$$A := \left[\int_\Omega (\nabla\varphi_j)^T \nabla\varphi_i + (\nabla\varphi_j)^T \boldsymbol{\beta}\varphi_i + \gamma\varphi_j\varphi_i\right]_{i,j=1}^N. \tag{87}$$

We are interested in the spectral distribution of the matrices in (87) in the case of hyperbolic and trigonometric tensor-product GB-splines.

For a compact and clean description of the results, throughout this section, we use the multi-index notation, see [33, Section 6] (or [15, Section 2.1]). A multi-index $\boldsymbol{m} \in \mathbb{Z}^d$ is a (row) vector in $\mathbb{Z}^d$ and its components are denoted by $m_1,\dots,m_d$. We indicate by $\mathbf{0}$, $\mathbf{1}$, $\mathbf{2}$ the vectors consisting of all zeros, all ones, all twos, respectively. We set $N(\boldsymbol{m}) := \prod_{i=1}^d m_i$ and $\boldsymbol{jk} := (j_1k_1,\dots,j_dk_d)$. The inequality $\boldsymbol{j} \leq \boldsymbol{k}$ means that $j_i \leq k_i$ for $i = 1,\dots,d$, and the multi-index range $\boldsymbol{j},\dots,\boldsymbol{k}$ is the set $\{\boldsymbol{i} \in \mathbb{Z}^d : \boldsymbol{j} \leq \boldsymbol{i} \leq \boldsymbol{k}\}$. We assume for this set the standard lexicographic ordering:

$$\Big[\ \dots\ \Big[\ [\ (i_1,\dots,i_d)\ ]_{i_d=j_d,\dots,k_d}\ \Big]_{i_{d-1}=j_{d-1},\dots,k_{d-1}}\ \dots\ \Big]_{i_1=j_1,\dots,k_1}. \tag{88}$$

We write $\boldsymbol{i} = \boldsymbol{j},\dots,\boldsymbol{k}$ to denote that the multi-index $\boldsymbol{i}$ varies in the multi-index range $\boldsymbol{j},\dots,\boldsymbol{k}$ taking all the values from $\boldsymbol{j}$ to $\boldsymbol{k}$ following the ordering in (88). For example, if $\boldsymbol{m} \in \mathbb{N}^d$ and $\mathbf{x} := [x_{\boldsymbol{i}}]_{\boldsymbol{i}=\mathbf{1}}^{\boldsymbol{m}}$, then $\mathbf{x}$ is a vector of length $N(\boldsymbol{m})$ whose components $x_{\boldsymbol{i}}$, $\boldsymbol{i} = \mathbf{1},\dots,\boldsymbol{m}$, are ordered according to (88): the first component is $x_{\mathbf{1}} = x_{(1,\dots,1,1)}$, the second component is $x_{(1,\dots,1,2)}$, and so on.

6.1 Multi-dimensional GB-spline basis functions and IgA Galerkin matrices

Let $\boldsymbol{p} := (p_1,\dots,p_d)$ and $\boldsymbol{n} := (n_1,\dots,n_d)$ be multi-indices such that $p_i \geq 2$, $n_i \geq 1$, $i = 1,\dots,d$. Let $\boldsymbol{U} := (U_1,\dots,U_d)$ and $\boldsymbol{V} := (V_1,\dots,V_d)$ be vectors of functions such that for $i = 1,\dots,d$ the pair of functions $\{U_i^{(p-1)}, V_i^{(p-1)}\}$ is a Chebyshev system on $[t_{i,j}, t_{i,j+1}]$, $j = p_i+1,\dots,p_i+n_i$, where

$$\{t_{i,1},\dots,t_{i,n_i+2p_i+1}\} := \Big\{\underbrace{0,\dots,0}_{p_i+1}, \frac{1}{n_i}, \frac{2}{n_i}, \dots, \frac{n_i-1}{n_i}, \underbrace{1,\dots,1}_{p_i+1}\Big\}.$$

The tensor-product GB-splines $N_{\boldsymbol{i},\boldsymbol{p}}^{\boldsymbol{U},\boldsymbol{V}} : [0,1]^d \to \mathbb{R}$ are defined by

$$N_{\boldsymbol{i},\boldsymbol{p}}^{\boldsymbol{U},\boldsymbol{V}} := N_{i_1,p_1}^{U_1,V_1} \otimes \cdots \otimes N_{i_d,p_d}^{U_d,V_d}, \quad \boldsymbol{i} = \boldsymbol{2},\dots,\boldsymbol{n}+\boldsymbol{p}-\boldsymbol{1}. \tag{89}$$

In the framework of IgA based on (uniform) GB-splines, the functions φ_i, $i = 1,\dots,N$, in (87) are chosen as the tensor-product GB-splines in (89), so that $N = N(\boldsymbol{n}+\boldsymbol{p}-\boldsymbol{2})$. We adopt for the tensor-product GB-splines (89) the lexicographic ordering[3] in (88), and we follow this ordering when assembling the matrix in (87), which from now on will be denoted by $A_{\boldsymbol{n},\boldsymbol{p}}^{\boldsymbol{U},\boldsymbol{V}}$. In multi-index notation it is expressed by

$$A_{\boldsymbol{n},\boldsymbol{p}}^{\boldsymbol{U},\boldsymbol{V}} = K_{\boldsymbol{n},\boldsymbol{p}}^{\boldsymbol{U},\boldsymbol{V}} + R_{\boldsymbol{n},\boldsymbol{p}}^{\boldsymbol{U},\boldsymbol{V}}, \tag{90}$$

where

$$K_{\boldsymbol{n},\boldsymbol{p}}^{\boldsymbol{U},\boldsymbol{V}} := \left[\int_{[0,1]^d} \left(\nabla N_{\boldsymbol{j}+\boldsymbol{1},\boldsymbol{p}}^{\boldsymbol{U},\boldsymbol{V}}\right)^T \nabla N_{\boldsymbol{i}+\boldsymbol{1},\boldsymbol{p}}^{\boldsymbol{U},\boldsymbol{V}}\right]_{\boldsymbol{i},\boldsymbol{j}=\boldsymbol{1}}^{\boldsymbol{n}+\boldsymbol{p}-\boldsymbol{2}}$$

is the matrix resulting from the discretization of the diffusive term in (86), and

$$R_{\boldsymbol{n},\boldsymbol{p}}^{\boldsymbol{U},\boldsymbol{V}} := \left[\int_{[0,1]^d} \left(\left(\nabla N_{\boldsymbol{j}+\boldsymbol{1},\boldsymbol{p}}^{\boldsymbol{U},\boldsymbol{V}}\right)^T \boldsymbol{\beta}\, N_{\boldsymbol{i}+\boldsymbol{1},\boldsymbol{p}}^{\boldsymbol{U},\boldsymbol{V}} + \gamma N_{\boldsymbol{j}+\boldsymbol{1},\boldsymbol{p}}^{\boldsymbol{U},\boldsymbol{V}} N_{\boldsymbol{i}+\boldsymbol{1},\boldsymbol{p}}^{\boldsymbol{U},\boldsymbol{V}}\right)\right]_{\boldsymbol{i},\boldsymbol{j}=\boldsymbol{1}}^{\boldsymbol{n}+\boldsymbol{p}-\boldsymbol{2}}$$

is the matrix resulting from the discretization of the terms in (86) with lower order derivatives. Moreover, it follows from (18)–(20) that

$$K_{\boldsymbol{n},\boldsymbol{p}}^{\boldsymbol{U},\boldsymbol{V}} = \sum_{i=1}^{d} \left(\bigotimes_{r=1}^{i-1} \frac{1}{n_r} M_{n_r,p_r}^{U_r,V_r}\right) \otimes n_i K_{n_i,p_i}^{U_i,V_i} \otimes \left(\bigotimes_{r=i+1}^{d} \frac{1}{n_r} M_{n_r,p_r}^{U_r,V_r}\right), \tag{91}$$

where for every $X \in \mathbb{C}^{m_1\times m_1}$ and $Y \in \mathbb{C}^{m_2\times m_2}$, the tensor product $X \otimes Y$ is the matrix in $\mathbb{C}^{m_1m_2\times m_1m_2}$ given by

$$X \otimes Y := \begin{bmatrix} x_{11}Y & x_{12}Y & \cdots & x_{1m_1}Y \\ x_{21}Y & x_{22}Y & \cdots & x_{2m_1}Y \\ \vdots & \vdots & & \vdots \\ x_{m_11}Y & x_{m_12}Y & \cdots & x_{m_1m_1}Y \end{bmatrix}.$$

Like in the one-dimensional setting, we denote by $A_{\boldsymbol{n},\boldsymbol{p}}^{\mathbb{Q}_{\boldsymbol{\mu}}}$ the stiffness matrix in (90) when hyperbolic or trigonometric GB-splines with parameters $\boldsymbol{\mu} := (\mu_1,\dots,\mu_d)$ are considered in (89). Note that different section spaces can be used in different directions.

[3] A different ordering has been used in [14] in the bivariate setting.

6.2 Multi-dimensional symbol of the normalized IgA Galerkin matrices

From now on, we assume that $n_i = \nu_i n \in \mathbb{N}$ for each $i = 1,\dots,d$, i.e., $\boldsymbol{n} = \boldsymbol{\nu} n$ for a fixed vector $\boldsymbol{\nu} := (\nu_1,\dots,\nu_d)$. The next two theorems provide the spectral distribution of the normalized stiffness matrices in the multi-dimensional setting, in the nested and in the non-nested case, respectively. These results are a consequence of the one-dimensional results in Lemma 5 and Theorems 5–6. They can be proved by using the same line of arguments as in [14, Theorem 18] and by taking into account (90)–(91). In both cases, we assume that $\boldsymbol{\alpha} := (\alpha_1,\dots,\alpha_d)$ is a suitable sequence of real, fixed parameters not depending on n.

Theorem 8 *The sequence of normalized matrices $\{n^{d-2} A^{\mathbb{Q}_\alpha}_{\boldsymbol{n},\boldsymbol{p}}\}_n$ is distributed, in the sense of the eigenvalues, like the function $f_{\boldsymbol{p},\boldsymbol{\nu}} : [-\pi,\pi]^d \to \mathbb{R}$,*

$$f_{\boldsymbol{p},\boldsymbol{\nu}}(\boldsymbol{\theta}) := \frac{1}{N(\boldsymbol{\nu})} \sum_{i=1}^{d} \nu_i^2 \Big(h_{p_1} \otimes \cdots \otimes h_{p_{i-1}} \otimes f_{p_i} \otimes h_{p_{i+1}} \otimes \cdots \otimes h_{p_d} \Big)(\boldsymbol{\theta}).$$

Theorem 9 *The sequence of normalized matrices $\{n^{d-2} A^{\mathbb{Q}_{n\alpha}}_{\boldsymbol{n},\boldsymbol{p}}\}_n$ is distributed, in the sense of the eigenvalues, like the function $f^{\mathbb{Q}_\alpha}_{\boldsymbol{p},\boldsymbol{\nu}} : [-\pi,\pi]^d \to \mathbb{R}$,*

$$f^{\mathbb{Q}_\alpha}_{\boldsymbol{p},\boldsymbol{\nu}}(\boldsymbol{\theta}) := \frac{1}{N(\boldsymbol{\nu})} \sum_{i=1}^{d} \nu_i^2 \Big(h^{\mathbb{Q}_{\alpha_1}}_{p_1} \otimes \cdots \otimes h^{\mathbb{Q}_{\alpha_{i-1}}}_{p_{i-1}} \otimes f^{\mathbb{Q}_{\alpha_i}}_{p_i} \otimes h^{\mathbb{Q}_{\alpha_{i+1}}}_{p_{i+1}} \otimes \cdots \otimes h^{\mathbb{Q}_{\alpha_d}}_{p_d} \Big)(\boldsymbol{\theta}).$$

Remark 14 Like in the univariate case, for nested GB-spline spaces (Theorem 8) the symbol is the same as for polynomial B-spline spaces, see [15, Eq. (4.18)].

Remark 15 From Theorems 8–9 and from Lemmas 2–3 we know that the symbols of the sequences $\{n^{d-2} A^{\mathbb{Q}_\alpha}_{\boldsymbol{n},\boldsymbol{p}}\}_n$, $\{n^{d-2} A^{\mathbb{Q}_{n\alpha}}_{\boldsymbol{n},\boldsymbol{p}}\}_n$ have a (theoretical) zero at $\boldsymbol{\theta} = \boldsymbol{0}$. Moreover, from (59) and Lemma 4 it follows that these symbols have also 'numerical zeros' for large $\boldsymbol{p}$ at the points $\boldsymbol{\theta} := (\theta_1,\dots,\theta_d)$ with $\theta_i = \pi$ for some i, see also Remarks 9 and 12. This peculiar behavior has already been pointed out for the (polynomial) B-spline case in [9,10,15]. We expect that the same unsatisfactory multigrid behavior described in Remark 10 also occurs in the multivariate hyperbolic/trigonometric GB-spline setting, with a possible multi-iterative remedy as suggested in Remark 11.

7 Conclusions

We have presented a spectral analysis of matrices arising from IgA Galerkin methods based on GB-splines, focusing on hyperbolic and trigonometric GB-splines because of their relevance in applications. A deep understanding of the spectral properties is a fundamental ingredient in the design of robust and optimal multigrid solvers for the corresponding linear systems.

The univariate setting has been investigated in detail. We have shown that the stiffness and mass matrices possess an asymptotic eigenvalue distribution when the matrix-size tends to infinity or, equivalently, the fineness parameter of the discretization tends to zero. This distribution is compactly described by a function (the symbol). The symbols in the hyperbolic, trigonometric and polynomial case are very similar, and they are exactly the same when considering sequences of nested spaces. Therefore, the corresponding sequences of GB-spline matrices present similar spectral features (in the nested and non-nested cases)

as the polynomial B-spline matrices. In particular, the symbols have a unique (theoretical) zero at $\theta = 0$. However, there is also an exponential decay to 0 at $\theta = \pi$ for large degrees, and this reveals the existence of a subspace of high frequencies where these matrices are ill-conditioned. This surprising fact has already been observed, analyzed, and exploited for designing robust and optimal multigrid solvers in the polynomial spline case, see [9, 10]. Thanks to the tensor-product structure of the approximation spaces, the univariate results extend directly to the multivariate setting.

The results on the spectral distribution of the stiffness and mass matrices have been used to analyze the performance of the spectral Galerkin approximation based on trigonometric B-splines for the univariate Laplace operator. It turns out that non-nested spaces are of particular interest in this context because their phase parameters can be fine-tuned to improve the relative spectral error according to user predefined criteria.

As a first step, we have only addressed problems with constant coefficients and no geometry map. Nevertheless, due to the similarity with the polynomial case, it is reasonable to expect that the general setting, with non-constant coefficients and geometry maps, can be treated with similar techniques as those used in the polynomial case starting from the univariate results [15].

The presented spectral analysis strengthens the similarity between classical (polynomial) B-splines and hyperbolic/trigonometric GB-splines, and confirms that B-splines and GB-splines are plug-to-plug compatible also from the linear algebra point of view.

Acknowledgements

This work was partially supported by INdAM-GNCS Gruppo Nazionale per il Calcolo Scientifico, by the MIUR 'Futuro in Ricerca 2013' Programme through the project DREAMS, and by the 'Uncovering Excellence' Programme of the University of Rome 'Tor Vergata' through the project DEXTEROUS.

References

1. Aricó, A., Donatelli, M., Serra-Capizzano, S.: *V-cycle optimal convergence for certain (multilevel) structured linear systems*. SIAM J. Matrix Anal. Appl. **26**, 186–214 (2004)
2. Beckermann, B., Kuijlaars, A.B.J.: *Superlinear convergence of conjugate gradients*. SIAM J. Numer. Anal. **39**, 300–329 (2001)
3. Beirão da Veiga, L., Buffa, A., Rivas, J., Sangalli, G.: *Some estimates for h-p-k-refinement in isogeometric analysis*. Numer. Math. **118**, 271–305 (2011)
4. Carnicer, J.M., Mainar, E., Peña, J.M.: *Critical length for design purposes and extended Chebyshev spaces*. Constr. Approx. **20**, 55–71 (2004)
5. Chui, C.K.: *An Introduction to Wavelets*. Academic Press (1992)
6. Costantini, P., Lyche, T., Manni, C.: *On a class of weak Tchebycheff systems*. Numer. Math. **101**, 333–354 (2005)
7. Cottrell, J.A., Hughes, T.J.R., Bazilevs, Y.: *Isogeometric Analysis: Toward Integration of CAD and FEA*. Wiley (2009)
8. Cottrell, J.A., Reali, A., Bazilevs, Y., Hughes, T.J.R.: *Isogeometric analysis of structural vibrations*. Comput. Methods Appl. Mech. Engrg. **195**, 5257–5296 (2006)
9. Donatelli, M., Garoni, C., Manni, C., Serra-Capizzano, S., Speleers, H.: *Robust and optimal multi-iterative techniques for IgA Galerkin linear systems*. Comput. Methods Appl. Mech. Engrg. **284**, 230–264 (2015)
10. Donatelli, M., Garoni, C., Manni, C., Serra-Capizzano, S., Speleers, H.: *Robust and optimal multi-iterative techniques for IgA collocation linear systems*. Comput. Methods Appl. Mech. Engrg. **284**, 1120–1146 (2015)

11. Donatelli, M., Garoni, C., Manni, C., Serra-Capizzano, S., Speleers, H.: *Spectral analysis and spectral symbol of matrices in isogeometric collocation methods*. Math. Comp. (To appear)
12. Donatelli, M., Garoni, C., Manni, C., Serra-Capizzano, S., Speleers, H.: *Symbol-based multigrid methods for Galerkin B-spline isogeometric analysis*. Tech. Report TW650, Dept. Computer Science, KU Leuven (2014)
13. Garoni, C., Hughes, T.J.R., Reali, A., Serra-Capizzano, S., Speleers, H.: *Smoothness versus polynomial degree: Why IgA outperforms FEA in the spectral approximation*. In preparation
14. Garoni, C., Manni, C., Pelosi, F., Serra-Capizzano, S., Speleers, H.: *On the spectrum of stiffness matrices arising from isogeometric analysis*. Numer. Math. **127**, 751–799 (2014)
15. Garoni, C., Manni, C., Serra-Capizzano, S., Sesana, D., Speleers, H.: *Spectral analysis and spectral symbol of matrices in isogeometric Galerkin methods*. Tech. Report 2015-005, Dept. Information Technology, Uppsala University (2015)
16. Garoni, C., Serra-Capizzano, S.: *The theory of generalized locally Toeplitz sequences: A review, an extension, and a few representative applications*. Tech. Report 2015-023, Dept. Information Technology, Uppsala University (2015)
17. Golinskii, L., Serra-Capizzano, S.: *The asymptotic properties of the spectrum of nonsymmetrically perturbed Jacobi matrix sequences*. J. Approx. Theory **144**, 84–102 (2007)
18. Grenander, U., Szegö, G.: *Toeplitz Forms and Their Applications*, Second Edition. Chelsea, New York (1984)
19. Hughes, T.J.R., Cottrell, J.A., Bazilevs, Y.: *Isogeometric analysis: CAD, finite elements, NURBS, exact geometry and mesh refinement*. Comput. Methods Appl. Mech. Engrg. **194**, 4135–4195 (2005)
20. Hughes, T.J.R., Evans, J.A., Reali, A.: *Finite Element and NURBS approximations of eigenvalue, boundary-value, and initial-value problems*. Comput. Methods Appl. Mech. Engrg. **272**, 290–320 (2014)
21. Kuijlaars, A.: *Convergence analysis of Krylov subspace iterations with methods from potential theory*. SIAM Review **48**, 3–40 (2006)
22. Kvasov, B.I., Sattayatham, P.: *GB-splines of arbitrary order*. J. Comput. Appl. Math. **104**, 63–88 (1999)
23. Manni, C., Pelosi, F., Sampoli, M.L.: *Generalized B-splines as a tool in isogeometric analysis*. Comput. Methods Appl. Mech. Engrg. **200**, 867–881 (2011)
24. Manni, C., Pelosi, F., Sampoli, M.L.: *Isogeometric analysis in advection-diffusion problems: Tension splines approximation*. J. Comput. Appl. Math. **236**, 511–528 (2011)
25. Manni, C., Reali, A., Speleers, H.: *Isogeometric collocation methods with generalized B-splines*. Comput. Math. Appl. **70**, 1659–1675 (2015)
26. Serra, S.: *Multi-iterative methods*. Comput. Math. Appl. **26**, 65–87 (1993)
27. Serra-Capizzano, S.: *The rate of convergence of Toeplitz based PCG methods for second order nonlinear boundary value problems*. Numer. Math. **81**, 461–495 (1999)
28. Serra-Capizzano, S.: *Generalized locally Toeplitz sequences: Spectral analysis and applications to discretized partial differential equations*. Linear Algebra Appl. **366**, 371–402 (2003)
29. Serra-Capizzano, S.: *The GLT class as a generalized Fourier analysis and applications*. Linear Algebra Appl. **419**, 180–233 (2006)
30. Serra-Capizzano, S., Tablino Possio, C.: *Analysis of preconditioning strategies for collocation linear systems*. Linear Algebra Appl. **369**, 41–75 (2003)
31. Serra-Capizzano, S., Tilli, P.: *On unitarily invariant norms of matrix-valued linear positive operators*. J. Taylor & Francis Group of Inequal. & Appl. **7**, 309–330 (2002)
32. Tilli, P.: *A note on the spectral distribution of Toeplitz matrices*. Linear Multilinear Algebra **45**, 147–159 (1998)
33. Tyrtyshnikov, E.E.: *A unifying approach to some old and new theorems on distribution and clustering.* Linear Algebra Appl. **232**, 1–43 (1996)
34. Unser, M., Blu, T.: *Cardinal exponential splines: Part I–theory and filtering algorithms*. IEEE Trans. Signal Proc. **53**, 1425–1438 (2005)
35. Wang, G., Fang, M.: *Unified and extended form of three types of splines*. J. Comput. Appl. Math. **216**, 498–508 (2008)